Chapter 6
Metal Matrix Composites

Metal matrix composites consist of a metal or an alloy as the continuous matrix and a reinforcement that can be particle, short fiber or whisker, or continuous fiber. In this chapter, we first describe important techniques to process metal matrix composites, then we describe the interface region and its characteristics, properties of different metal matrix composites, and finally, we summarize different applications of metal matrix composites.

6.1 Types of Metal Matrix Composites

There are three kinds of metal matrix composites (MMCs):

- Particle reinforced MMCs
- Short fiber or whisker reinforced MMCs
- Continuous fiber or sheet reinforced MMCs

Table 6.1 provides examples of some important reinforcements used in metal matrix composites and their aspect (length/diameter) ratios and diameters. Particle or discontinuously reinforced MMCs have become very important because they are inexpensive vis à vis continuous fiber reinforced composites and they have relatively isotropic properties compared to fiber reinforced composites. Figure 6.1a, b show typical microstructures of continuous alumina fiber/magnesium alloy and silicon carbide particle/aluminum alloy composites, respectively. Use of nanometer-sized fullerenes as a reinforcement has been tried. In addition to being very small, fullerenes (of which C_{60} is the most common) are light and hollow. The important question in this regard is whether they remain stable during processing and service. For the interested reader, we cite work by Barrera et al. (1994), who used powder metallurgy, RF sputtering of a composite

K.K. Chawla, *Composite Materials: Science and Engineering*,
DOI 10.1007/978-0-387-74365-3_6,

(multifullerene) target, and thin film codeposition methods to make fullerene/metal composites. Copper–fullerene composites were processed by sputtering copper during fullerene sublimation in an argon atmosphere. Fullerenes were found to withstand the processing. However, in the case of aluminum matrix, brittle Al_4C_3 was observed to form at high temperatures.

Table 6.1 Typical reinforcements used in metal matrix composites

Type	Aspect ratio	Diameter (μm)	Examples
Particle	~1–4	1–25	SiC, Al_2O_3, WC, TiC, BN, B_4C
Short fiber or whisker	~10–1,000	0.1–25	SiC, Al_2O_3, Al_2O_3 + SiO_2, C
Continuous fiber	>1,000	3–150	SiC, Al_2O_3, Al_2O_3 + SiO_2, C, B, W, NbTi, Nb_3Sn

6.2 Important Metallic Matrices

A variety of metals and their alloys can be used as matrix materials. We describe briefly the important characteristics of some of the more common ones.

6.2.1 Aluminum Alloys

Aluminum alloys, because of their low density and excellent strength, toughness, and resistance to corrosion, find important applications in the aerospace field. Of special mention in this regard are the Al–Cu–Mg and Al–Zn–Mg–Cu alloys, very important precipitation-hardenable alloys. Aluminum-lithium alloys form one of the most important precipitation-hardenable aluminum alloys. Lithium, when added to aluminum as a primary alloying element, has the unique characteristic of increasing the elastic modulus and decreasing the density of the alloy. Understandably, the aerospace industry has been the major target of this development. Al–Li alloys are precipitation hardenable, much like the Al–Cu–Mg and Al–Zn–Mg–Cu alloys. The precipitation hardening sequence in Al–Li alloys is, however, much more complex than that observed in conventional precipitation-hardenable aluminum alloys. Generally, these alloys contain, besides lithium, some copper, zirconium, and magnesium. Vasudevan and Doherty (1989) provide an account of the heat treatments and structure/property aspects of various aluminum alloys.

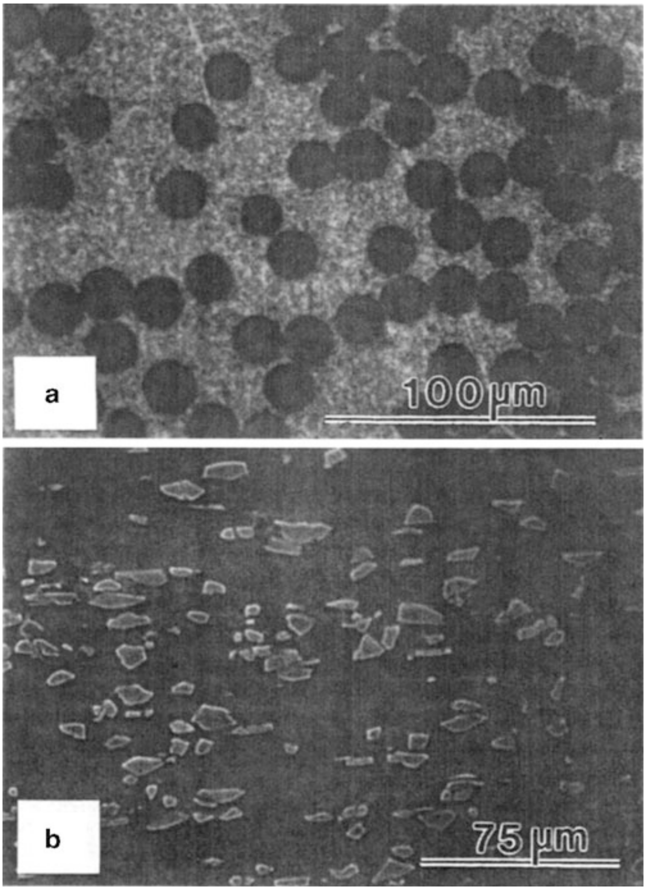

Fig. 6.1 (**a**) Transverse cross-section of continuous alumina fiber/magnesium alloy composite. (**b**) Typical microstructure of a silicon carbide particle/aluminum alloy composite. Note the angular nature of SiC particles and alignment of particles along the long axis

6.2.2 Titanium Alloys

Titanium is one of the important aerospace materials. It has a density of 4.5 g/cm^3 and a Young's modulus of 115 GPa. For titanium alloys, the density can vary between 4.3 and 5.1 g/cm^3, while the modulus can have a range of 80–130 GPa. High strength/weight and modulus/weight ratios are important. Titanium has a relatively high melting point (1,672°C) and retains strength to high temperatures with good oxidation and corrosion resistance. All these factors make it an ideal material for aerospace applications. Titanium alloys are used in jet engines (turbine and compressor blades), fuselage parts, etc. It is, however, an expensive material.

At supersonic speeds, the skin of an airplane heats up so much that aluminum alloys are no good; titanium alloys must be used at such high temperatures. At speeds greater than Mach 2, the temperatures will be even higher than what titanium alloys can withstand. Titanium aluminides are one of the candidate materials in this case.

Titanium has two polymorphs: alpha (α) titanium has a hexagonal close-packed (hcp) structure and is stable below 885°C and beta (β) titanium has a bcc structure and is stable above 885°C. Aluminum raises the $\alpha \rightarrow \beta$ transformation temperature, i.e., aluminum is an alpha stabilizer. Most other alloying elements (Fe, Mn, Cr, Mo, V, No, Ta) lower the $\alpha \rightarrow \beta$ transformation temperature, i.e., they stabilize the β phase. Thus, three general alloy types can be produced, viz., α, α + β, and β titanium alloys. The Ti-6%Al-4% V, called the *workhorse* Ti alloy of the aerospace industry, belongs to the α + β group. Most titanium alloys are not used in a quenched and tempered condition. Generally, hot working in the α + β region is carried out to break the structure and distribute the α phase in an extremely fine form.

Titanium has a great affinity for oxygen, nitrogen, and hydrogen. Parts per million of such interstitials in titanium can change mechanical properties drastically; particularly embrittlement can set in. That is why welding of titanium by any technique requires protection from the atmosphere. Electron beam techniques, in a vacuum, are frequently used.

6.2.3 Magnesium Alloys

Magnesium and its alloys form another group of very light materials. Magnesium is one of the lightest metals; its density is 1.74 g/cm^3. Magnesium alloys, especially castings, are used in aircraft gearbox housings, chain saw housings, electronic equipment, etc. Magnesium, being a hexagonal close-packed metal, is difficult to cold work.

6.2.4 Copper

Copper has a face centered cubic structure. Its use as an electrical conductor is quite ubiquitous. It has good thermal conductivity. It can be cast and worked easily. One of the major applications of copper in a composite as a matrix material is in niobium-based superconductors.

6.2.5 Intermetallic Compounds

Intermetallic compounds can be ordered or disordered. The structure of ordered intermetallic alloys is characterized by long-range ordering, i.e., different atoms occupy specific positions in the lattice. Because of their ordered structure, the motion of dislocations in intermetallics is much more restricted than in disordered alloys. This results in retention (in some cases, even an increase) of strength at elevated temperatures, a very desirable feature. For example, nickel aluminide shows a marked increase in strength up to 800°C. An undesirable feature of intermetallics is their extremely low ductility. Attempts at ductility enhancement in intermetallics have involved a number of metallurgical techniques. Rapid solidification is one method. Another technique that has met success is the addition of boron to Ni_3Al. With extremely small amounts of boron (0.06 wt.%), the ductility increases from about 2% to about 50%. Long-range order also has significant effects on diffusion-controlled phenomena such as recovery, recrystallization, and grain growth. The activation energy for these processes is increased, and these processes are slowed down. Thus, ordered intermetallic compounds tend to exhibit high creep resistance. Enhancing toughness by making composites with intermetallic matrix materials is a potential possibility.

An important disordered intermetallic is molybdenum disilicide ($MoSi_2$) (Vasudevan and Petrovic, 1992). It has a high melting point and shows good stability at temperatures greater than 1,200°C in oxidizing atmosphere. It is commonly used as a heating element in furnaces. The high oxidation resistance comes from a protective SiO_2 film that it tends to form at high temperatures.

6.3 Processing

Many processes for fabricating metal matrix composites are available. For the most part, these processes involve processing in the liquid and solid state. Some processes may involve a variety of deposition techniques or an in situ process of incorporating a reinforcement phase. We provide a summary of these fabrication processes.

6.3.1 Liquid-State Processes

Metals with melting temperatures that are not too high, such as aluminum, can be incorporated easily as a matrix by liquid route. A description of some important liquid-state processes is given here.

Casting, or *liquid infiltration*, involves infiltration of a fiber bundle by liquid metal (Divecha et al. 1981; Rohatgi et al. 1986). It is not easy to make MMCs by simple liquid-phase infiltration, mainly because of difficulties with wetting of ceramic reinforcement by the molten metal. When the infiltration of a fiber preform occurs readily, reactions between the fiber and the molten metal can significantly degrade fiber properties. Fiber coatings applied prior to infiltration, which improve wetting and control reactions, have been developed and can result in some improvements. In this case, however, the disadvantage is that the fiber coatings must not be exposed to air prior to infiltration because surface oxidation will alter

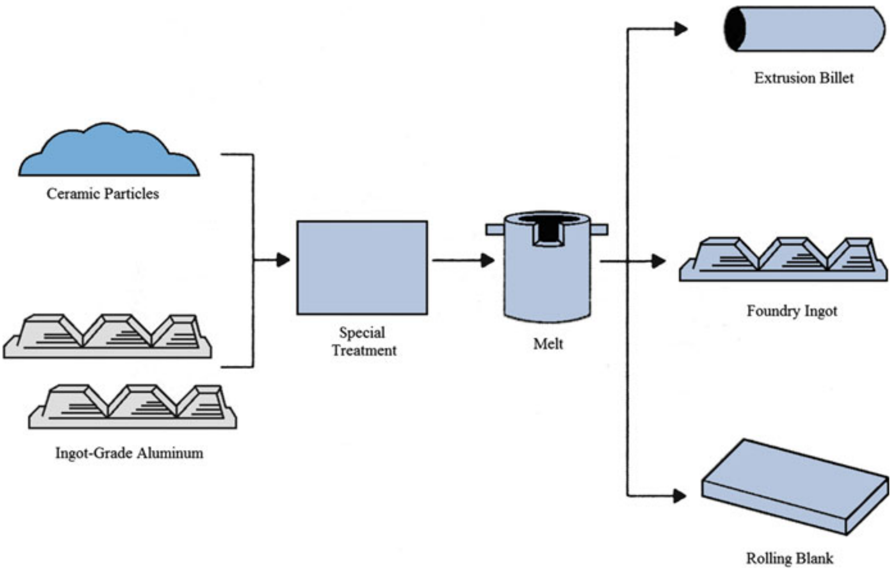

Fig. 6.2 Schematic of the Duralcan process

the positive effects of coating (Katzman 1987). One commercially successful liquid infiltration process involving particulate reinforcement is the *Duralcan* process. Figure 6.2 shows a schematic of this process. Ceramic particles and ingot-grade aluminum are mixed and melted. The ceramic particles are given a proprietary treatment. The melt is stirred just above the liquidus temperature—generally between 600 and 700°C. The melt is then converted into one of the following four forms: extrusion blank, foundry ingot, rolling bloom, or rolling ingot. The Duralcan process of making particulate composites by liquid metal casting involves the use of 8–12 μm particles. Too small particles, e.g., 2–3 μm, will result in a very large interface region and thus a very viscous melt. In foundry-grade MMCs, high Si aluminum alloys (e.g., A356) are used, while in wrought MMC, Al–Mg type alloys (e.g., 6061) are used. Alumina particles are typically used in foundry alloys, while silicon carbide particles are used in the wrought aluminum alloys.

For making continuous fiber reinforced MMCs, tows of fibers are passed through a liquid metal bath, where the individual fibers are wet by the molten metal, excess metal is wiped off, and a composite wire is produced. Figure 6.3 shows a micrograph of one such wire made of SiC fibers in an aluminum matrix. Note the multifiber cross sections in the broken composite wire. A bundle of such wires can be consolidated by extrusion to make a composite. Another pressureless liquid-metal infiltration process of making MMCs is Lanxide's Primex™ process, which can be used with certain reactive metal alloys such Al–Mg to infiltrate ceramic preforms. For an Al–Mg alloy, the process takes place between 750 and 1,000°C in a nitrogen-rich atmosphere (Aghajanian et al. 1989). Typical infiltration rates are less than 25 cm/h.

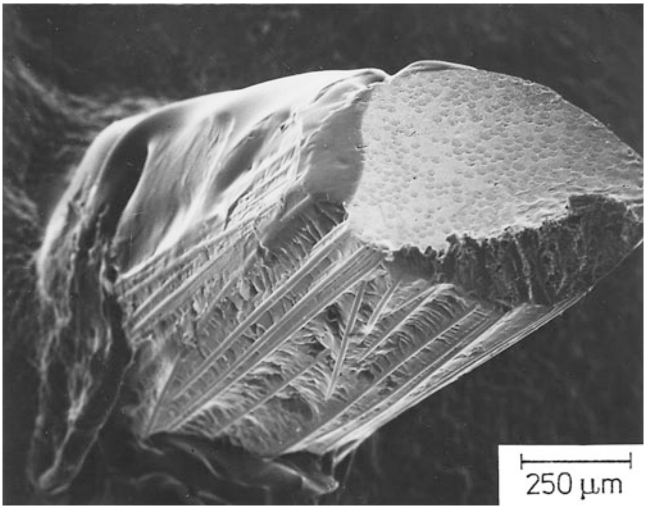

Fig. 6.3 A silicon carbide fiber/aluminum wire preform. SiC fibers can be seen in the transverse section as well as along the length the wire preform

Squeeze casting, or *pressure infiltration*, involves forcing the liquid metal into a fibrous preform. Figure 6.4 shows two processes of making a fibrous preform. In the press forming process, an aqueous slurry of fibers is well agitated and poured into a mold, pressure is applied to squeeze the water out, and the preform is dried (Fig. 6.4a). In other process, suction is applied to a well-agitated mixture of whisker, binder, and water. This is followed by demolding and drying of the fiber preform (Fig. 6.4b). A schematic of the squeeze casting process is shown in Fig. 6.5a. Pressure is applied until the solidification is complete. By forcing the molten metal through small pores of fibrous preform, this method obviates the requirement of good wettability of the reinforcement by the molten metal. Figure 6.5b shows the microstructure of Saffil alumina fiber/aluminum matrix composite made by squeeze casting. Composites fabricated with this method have minimal reaction between the reinforcement and molten metal because of short dwell time at high temperature and are free from common casting defects such as porosity and shrinkage cavities. Squeeze casting is really an old process, also called *liquid metal forging* in earlier versions. It was developed to obtain pore-free, fine-grained aluminum alloy components with superior properties than conventional permanent mold casting. In particular, the process has been used in the case of aluminum alloys that are difficult to cast by conventional methods, for example, silicon-free alloys used in diesel engine pistons where high-temperature strength is required. Inserts of nickel-containing cast iron, called Ni-resist, in the upper groove area of pistons have also been produced by the squeeze casting technique to provide wear resistance. Use of ceramic fiber reinforced metal matrix composites at locations of high wear and high thermal stress has resulted in a product much superior to the Ni-resist cast iron inserts.

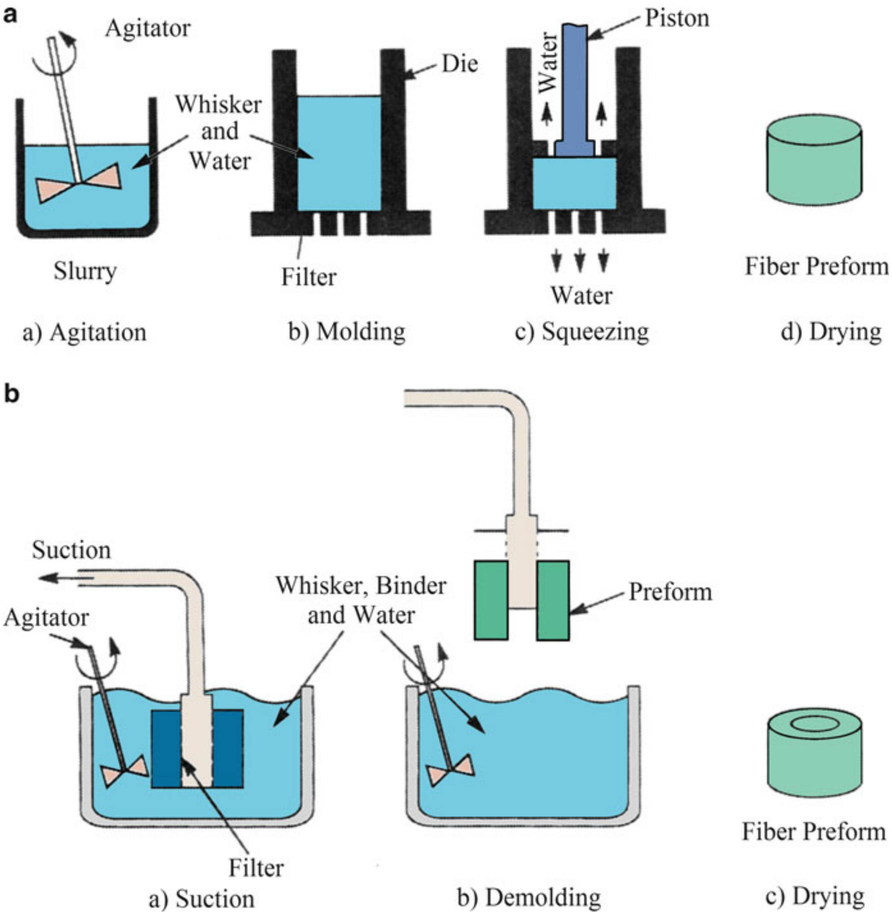

Fig. 6.4 (**a**) Press forming of a preform. (**b**) Suction forming of a preform

The squeeze casting technique, shown in Fig. 6.5a, has been quite popular in making composites with selective reinforcement. A porous fiber preform (generally of discontinuous Saffil-type Al_2O_3 fibers) is inserted into the die. Molten metal (aluminum) is poured into the preheated die located on the bed of a hydraulic press. The applied pressure (70–100 MPa) makes the molten aluminum penetrate the fiber preform and bond the fibers. Infiltration of a fibrous preform by means of a pressurized inert gas is another variant of liquid metal infiltration technique. The process is conducted in the controlled environment of a pressure vessel and rather high fiber volume fractions; complex-shaped structures are obtainable (Mortensen et al. 1988; Cook and Warner 1991). Although commonly, aluminum matrix composites are made by this technique, alumina fiber reinforced intermetallic matrix composites (e.g., TiAl, Ni_3Al, and Fe_3Al matrix materials) have been prepared by pressure casting (Nourbakhsh et al. 1990). The technique involves melting the matrix alloy in a crucible in vacuum, while the fibrous preform is heated separately. The molten matrix

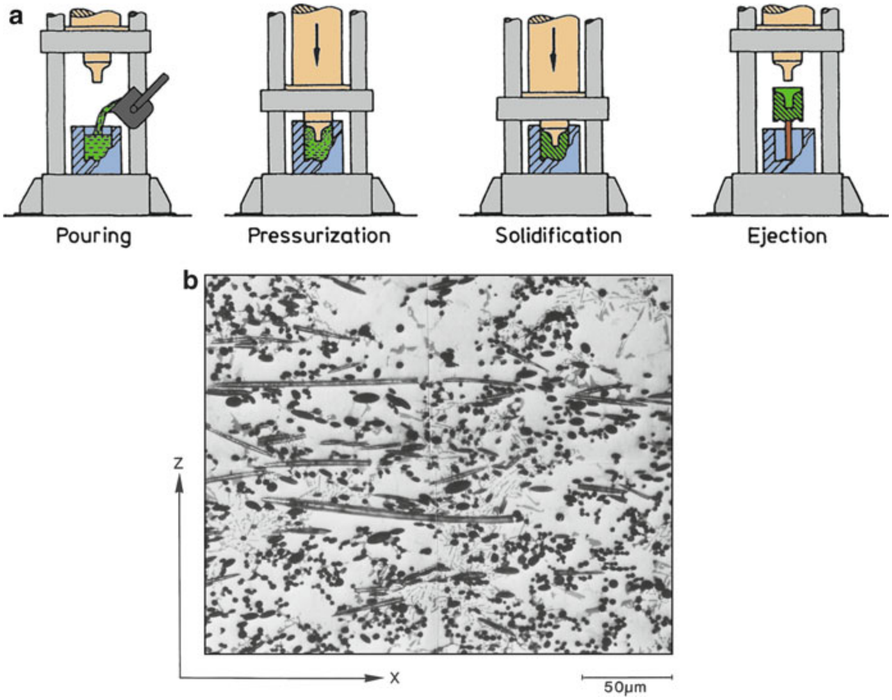

Fig. 6.5 (**a**) Squeeze casting technique of making a metal matrix composite. (**b**) The microstructure of Saffil alumina fiber/aluminum matrix composite made by squeeze casting. [Courtesy of G. Eggeler]

material (at about 100°C above the T_m) is poured onto the fibers, and argon gas is introduced simultaneously. Argon gas pressure forces the melt to infiltrate the preform. The melt generally contains additives to aid in wetting the fibers.

6.3.1.1 Special Issues in Casting of MMCs

Casting of metal matrix composites consisting of a metal containing particulate or fibrous reinforcement may appear to be superficially similar to casting of metals. Metals can be cast into near net-shape product forms because of their relatively low melt viscosities. In particular, when a metal is heated above its melting point (or in the case of an alloy above its liquidus temperature), we get a low-viscosity liquid that has nice fluid flow characteristics such that it can be used to infiltrate a fibrous or particulate preform (Michaud 1993; Cornie et al. 1986). Darcy's law describes the phenomenon of permeability of porous medium by a fluid. Specifically, in the case of MMCs, we can write for the permeability of a porous medium, k, in terms of Darcy's Law for single-phase fluid flow:

$$J = -\frac{k}{\eta}\nabla P,$$

where J is volume current density (i.e., volume/area × time) of the fluid, η is the fluid viscosity, and ∇P is the pressure gradient responsible for the fluid flow. One can immediately see that increasing the external pressure and/or decreasing the viscosity of the liquid will increase the volume current density, J.

Liquid phase processing of MMCs, more specifically, casting of aluminum matrix containing ceramic particles, one of the popular systems, requires some modifications to conventional aluminum casting processes, which are summarized as follows:

- Molten aluminum and silicon carbide can react and form Al_4C_3, an undesirable reaction product. Aluminum alloys that minimize reactivity with SiC should be used. Al–Si alloys (with Si levels of up to 9%) are typically used with SiC reinforcement. With increasing temperature, an increase in the amount of silicon is required to prevent Al_4C_3 formation.
- Covering the melt with an inert gas atmosphere will reduce oxidation of the melt.
- Addition of reinforcement particles increases the viscosity of the melt. Several equations have been proposed for the viscosity, η_c of particulate composite. The Einstein equation for dilute suspensions of spherical particles is well known, but it is valid for particle concentrations less than 0.1. The Einstein equation is

  $$\eta_c = \eta_m\left(1 + 2.5V_p\right),$$

  where η_m is the viscosity of the unreinforced metal and V_p is the volume fraction of particles. Another expression for the viscosity of a viscous melt containing particles is given by (Thomas 1965):

  $$\eta_c = \eta_m\left(1 + 2.5V_p + 10.05V_p^2\right).$$

  Thus, the temperature of the composite melt should be above a certain limit (~745°C for Al–Si/SiC) to keep the melt from becoming highly viscous.
- Stirring of the composite melt is required (Mehrabian et al. 1974). The density of SiC (3.2 g/cm^3) is higher than that of Al (2.5 g/cm^3), so the particles will sink unless the melt is agitated. Alternating currents in a magnetic field (Katsura 1982) and mechanical vibration (Pennander and Anderson 1991) have also been used to improve wetting and permeability of the reinforcement in the liquid matrix.

6.3.1.2 Centrifugal Casting

One of the disadvantages of MMCs with ceramic reinforcement is that they are typically more difficult to machine than the unreinforced alloy. In centrifugal casting, optimal placement of the reinforcement can be achieved by inducing a centrifugal force immediately during casting which allows one to intentionally obtain a gradient in reinforcement volume fraction (Divecha et al. 1981). Figure 6.6

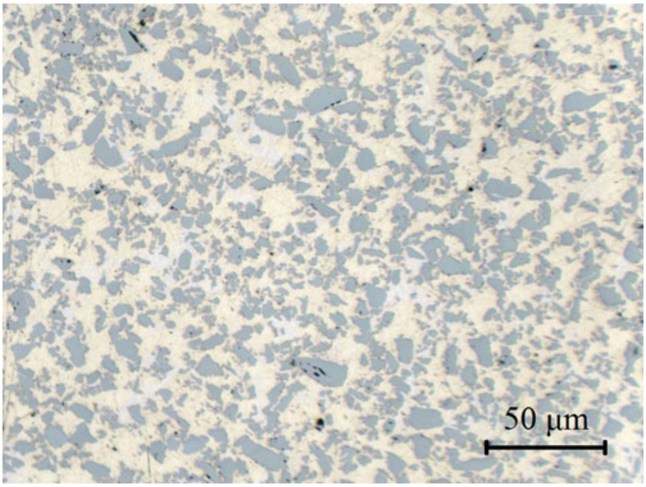

Fig. 6.6 Microstructure of a centrifugally cast WC/bronze composite

shows the microstructure of a centrifugally cast WC particle/bronze matrix composite. In brake rotors, for example, wear resistance is needed on the rotor face, but not in the hub area. Thus, in areas where reinforcement is not as crucial, such as in the hub area, easier machining may be obtained.

6.3.1.3 Processing of WC/Co Composites

Tungsten carbide (WC)/cobalt (Co) composites, commonly referred to as cemented carbides, are produced by powder processing. Even though powders are the starting materials in this process, we include this under the liquid phase processing category because pressureless, liquid phase sintering is used to form the metal matrix in this composite. This is because liquid cobalt wets WC particles very easily; it has a contact angle of zero degree with WC. Tungsten carbide particles are blended with cobalt powder by milling with an organic liquid to minimize heating and prevent oxidation. After milling, the liquid is removed by a spray-drying process, resulting in free-flowing, spherical granules of WC/Co. These granules are compacted under a pressure in the range of 50–150 MPa, which results in green compacts having 65% of the theoretical density. This is followed by pressureless, liquid phase sintering. Good infiltration of WC particles by liquid cobalt occurs because of capillary action and enhanced interfacial diffusion. A high density composite, accompanied by large amount shrinkage, is obtained. The capillary action results in some rearrangement of particles, leading to a closer packing of WC particles in Co matrix.

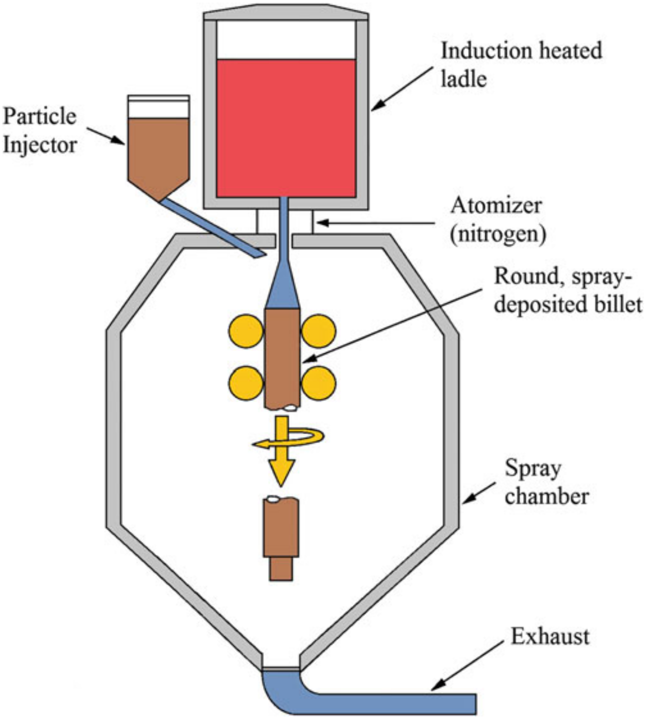

Fig. 6.7 Schematic of the spray forming process

6.3.1.4 Spray-Forming

Spray-forming of particulate MMCs involves the use of spray techniques that have been used for some time to produce monolithic alloys (Srivatsan and Lavernia 1992). A spray gun is used to atomize a molten aluminum alloy matrix. Ceramic particles, such as silicon carbide, are injected into this stream. Usually, the ceramic particles are preheated to dry them. Figure 6.7 shows a schematic of this process. An optimum particle size is required for an efficient transfer. Whiskers, for example, are too fine to be transferred. The preform produced in this way is generally quite porous. The cosprayed metal matrix composite is subjected to scalping, consolidation, and secondary finishing processes, thus making it a wrought material. The process is totally computer-controlled and quite fast. It also should be noted that the process is essentially a liquid metallurgy process. One avoids the formation of deleterious reaction products because the time of flight is extremely short. Silicon carbide particles of an aspect ratio (length/diameter) between 3 and 4 and volume fractions up to 20% have been incorporated into aluminum alloys. A great advantage of the process is the flexibility that it affords in making different types of composites. For example, one can make in situ laminates using two sprayers or one can have selective reinforcement. This process, however, is quite expensive, mainly because of the high cost of the capital equipment.

6.3.1.5 Modeling of Infiltration

When a metal is heated above its melting point (or in the case of an alloy above the liquidus temperature), we get a low-viscosity liquid that has nice fluid flow characteristics so that it can be used to infiltrate a fibrous preform (Michaud 1993; Cornie et al. 1986). Such an infiltration process can be described by phenomena such as capillarity and permeability. The phenomenon of permeability of a porous medium by a fluid is very important in a variety of fields. Specifically, in the case of MMCs, it is useful to be able to understand the permeability of a porous fibrous or particulate preform by the molten metal. Permeability of a porous medium, k, is commonly described by Darcy's law:

$$J = -\frac{k}{\eta}\nabla P,$$

where J is volume current density (i.e., volume/area × time) of the fluid, η is the fluid viscosity, and P is the pressure that drives the fluid flow. It can be recognized that Darcy's law is an analog of Ohm's law for electrical conduction, i.e., hydraulic permeability is an analog of electrical conductivity. Note that the permeability, k, is a function of the properties of the porous medium, i.e., its microstructure; it does not depend on properties of the fluid.

6.3.2 Solid State Processes

Many solid state techniques are available (Ghosh 1993). We describe some of the important ones.

Diffusion bonding is a common solid state welding technique used to join similar or dissimilar metals. Interdiffusion of atoms from clean metal surfaces in contact at an elevated temperature leads to welding. There are many variants of the basic diffusion bonding process; however, all of them involve a step of simultaneous application of pressure and high temperature. Matrix alloy foil and fiber arrays, composite wire, or monolayer laminae are stacked in a predetermined order. Figure 6.8a shows a schematic of one such diffusion bonding process, also called the *foil-fiber-foil process*. Figure 6.8b shows the microstructure of SiC fiber/titanium matrix composite made by diffusion bonding. The starting materials in this case were made by sputter coated SiC fibers with titanium. Filament winding was used to obtain panels, about 250 μm thick. Four such panels were stacked and hot pressed at 900°C, under a pressure of 105 MPa for 3 h. A careful examination of Fig. 6.8b will show the reader interfaces between sheets of Ti alloy matrix. Vacuum hot pressing is a most important step in the diffusion bonding processes for metal matrix composites. The major advantages of this technique are: the ability to process a wide variety of matrix metals and control of fiber orientation and volume fraction. Among the disadvantages are: processing times of several hours, high processing temperatures and pressures, all of which make the process quite expensive; besides the fact only objects of limited size can be produced. Hot isostatic pressing (HIP),

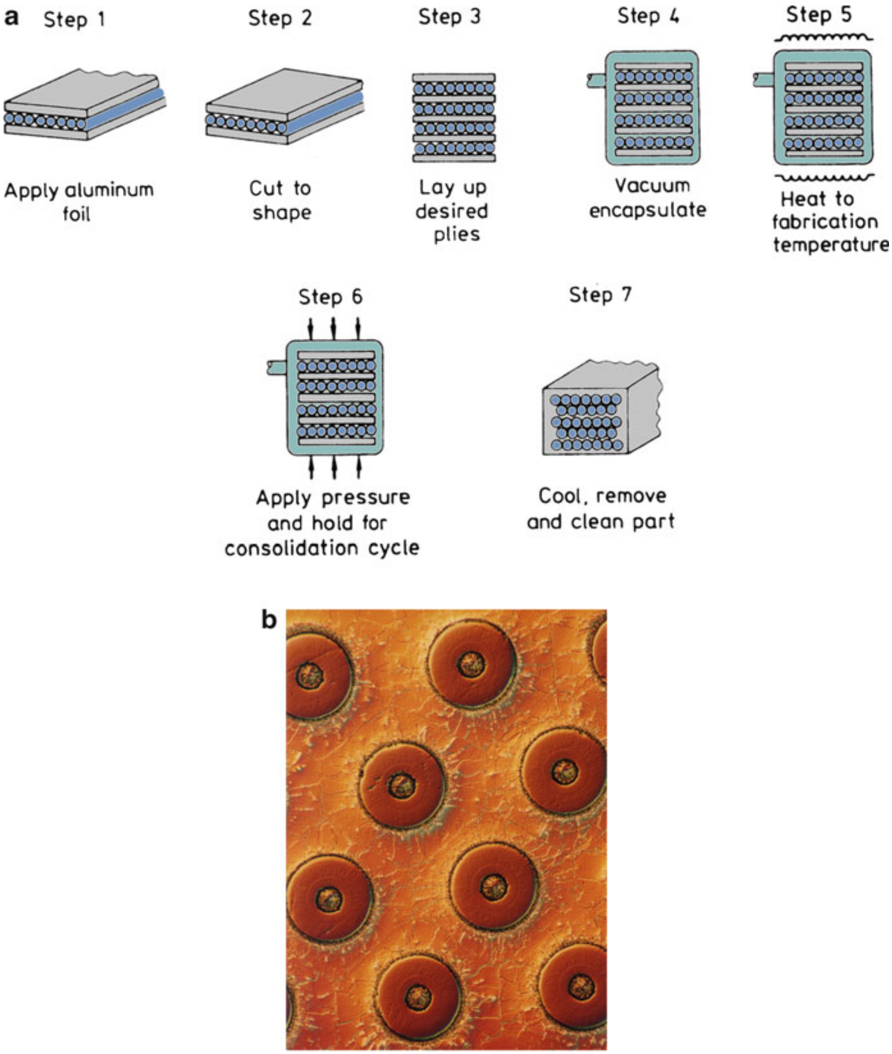

Fig. 6.8 (**a**) Schematic of diffusion bonding process. (**b**) The microstructure of SiC fiber/titanium matrix composite made by diffusion. Each fiber is 142 μm in diameter. [Courtesy of J. Baughman]

instead of uniaxial pressing, can also be used. In HIP, gas pressure against a can consolidates the composite piece contained inside the can. With HIP, it is relatively easy to apply high pressures at elevated temperatures over variable geometries.

Deformation processing of metal/metal composites involves mechanical processing (swaging, extrusion, drawing, or rolling) of a ductile two-phase material. The two phases codeform, causing the minor phase to elongate and become fibrous in nature within the matrix. These materials are sometimes referred to as *in situ composites*. The properties of a deformation-processed composite depend largely on the characteristics of the starting material, which is usually a billet of two-phase alloy that has been prepared by casting or powder metallurgy methods. Roll bonding is a common technique used to produce a laminated composite consisting of different metals in the sheet form (Chawla and Collares 1978; Sherby et al. 1985). Such composites are called sheet laminated metal matrix composites. Other examples of deformation-processed metal matrix composites are the niobium-based conventional filamentary superconductors and the high-T_c superconductors (see Chap. 9).

Deposition techniques for metal matrix composite fabrication involve coating individual fibers in a tow with the matrix material needed to form the composite followed by diffusion bonding to form a consolidated composite plate or structural shape. The main disadvantage of using deposition techniques is that they are very time consuming. However, there are several advantages:

- The degree of interfacial bonding is easily controllable; interfacial diffusion barriers and compliant coatings can be formed on the fiber prior to matrix deposition or graded interfaces can be formed.
- Thin, monolayer tapes can be produced by filament winding; these are easier to handle and mold into structural shapes than other precursor forms—unidirectional or angle-plied composites can be easily fabricated in this way.

Several deposition techniques are available: immersion plating, electroplating, spray deposition, chemical vapor deposition (CVD), and physical vapor deposition (PVD) (Partridge and Ward-Close 1993). Dipping or immersion plating is similar to infiltration casting except that fiber tows are continuously passed through baths of molten metal, slurry, sol, or organometallic precursors. Electroplating produces a coating from a solution containing the ion of the desired material in the presence of an electric current. Fibers are wound on a mandrel, which serves as the cathode, and placed into the plating bath with an anode of the desired matrix material. The advantage of this method is that the temperatures involved are moderate and no damage is done to the fibers. Problems with electroplating involve void formation between fibers and between fiber layers, adhesion of the deposit to the fibers may be poor, and there are limited numbers of alloy matrices available for this processing. A spray deposition operation, typically, consists of winding fibers onto a foil-coated drum and spraying molten metal onto them to form a monotape. The source of molten metal may be powder or wire feedstock, which is melted in a flame, arc, or plasma torch. The advantages of spray deposition are easy control of fiber alignment and rapid solidification of the molten matrix. In a CVD process, a vaporized component decomposes or reacts with another vaporized chemical on the substrate to form a coating on that substrate. The processing is generally carried out at elevated temperatures.

6.3.3 In Situ Processes

In in situ techniques, one forms the reinforcement phase in situ. The composite material is produced in one step from an appropriate starting alloy, thus avoiding the difficulties inherent in combining the separate components as in a typical composite processing. Controlled unidirectional solidification of a eutectic alloy is a classic example of in situ processing. Unidirectional solidification of a eutectic alloy can result in one phase being distributed in the form of fibers or ribbons in the other. One can control the fineness of distribution of the reinforcement phase by simply controlling the solidification rate. The solidification rate in practice, however, is limited to a range of 1–5 cm/h because of the need to maintain a stable growth front. The stable growth front requires a high temperature gradient. Figure 6.9 shows scanning electron micrographs of transverse sections of in situ composites obtained at different solidification rates (Walter 1982). The nickel alloy matrix has been etched away to reveal the TaC fibers. At low solidification rates, the TaC fibers are square in cross section, while at higher solidification rates, blades of TaC form. The number of fibers per square centimeter also increased with increasing solidification rate. Table 6.2 gives some important systems that have been investigated. A precast and homogenized rod of a eutectic composition is melted, in a vacuum or inert gas atmosphere. The rod is contained in a graphite crucible, which in turn is contained in a quartz tube. Heating is generally done by induction. The coil is moved up the quartz tube at a fixed rate. Thermal gradients can be increased by chilling the crucible just below the induction coil. Electron beam heating can also be used, especially when reactive metals such as titanium are involved. The reader is referred to McLean (1983).

The XD™ process is another in situ process; in this an exothermic reaction between two components is used to produce a third component. Sometimes such processing techniques are referred to as the *self-propagating high-temperature synthesis* (SHS) process. Specifically, the XD™ process produces ceramic particle reinforced metallic alloy. Generally, a master alloy containing rather high volume fraction of reinforcement is produced by the reaction synthesis. This is mixed and remelted with the base alloy to produce a desirable amount of particle reinforcement. Typical reinforcements are SiC, TiB_2, etc. in an aluminum, nickel, or intermetallic matrix (Christodolou et al. 1988).

6.4 Interfaces in Metal Matrix Composites

As we have repeatedly pointed out, the interface region in any composite is very important in determining the ultimate properties of the composite. In this section, we give examples of the microstructure of the interface region in different metal matrix composite systems and discuss the implications of various interfacial characteristics on the resultant properties of the composite. Recall that we can use contact angle, θ as a measure of wettability; a small θ indicates good wetting. Most often, the ceramic reinforcement is rejected by the molten metal because of nonwettability or high contact angle. Sometimes the contact angle of a liquid drop on a solid substrate can be decreased by increasing the surface energy of the solid (γ_{SV}) or by decreasing the energy of the interface between the liquid and the solid (γ_{SL}). Thus, under certain circumstances, the wettability of a solid ceramic by a molten metal can be improved by making a small alloy addition to the matrix

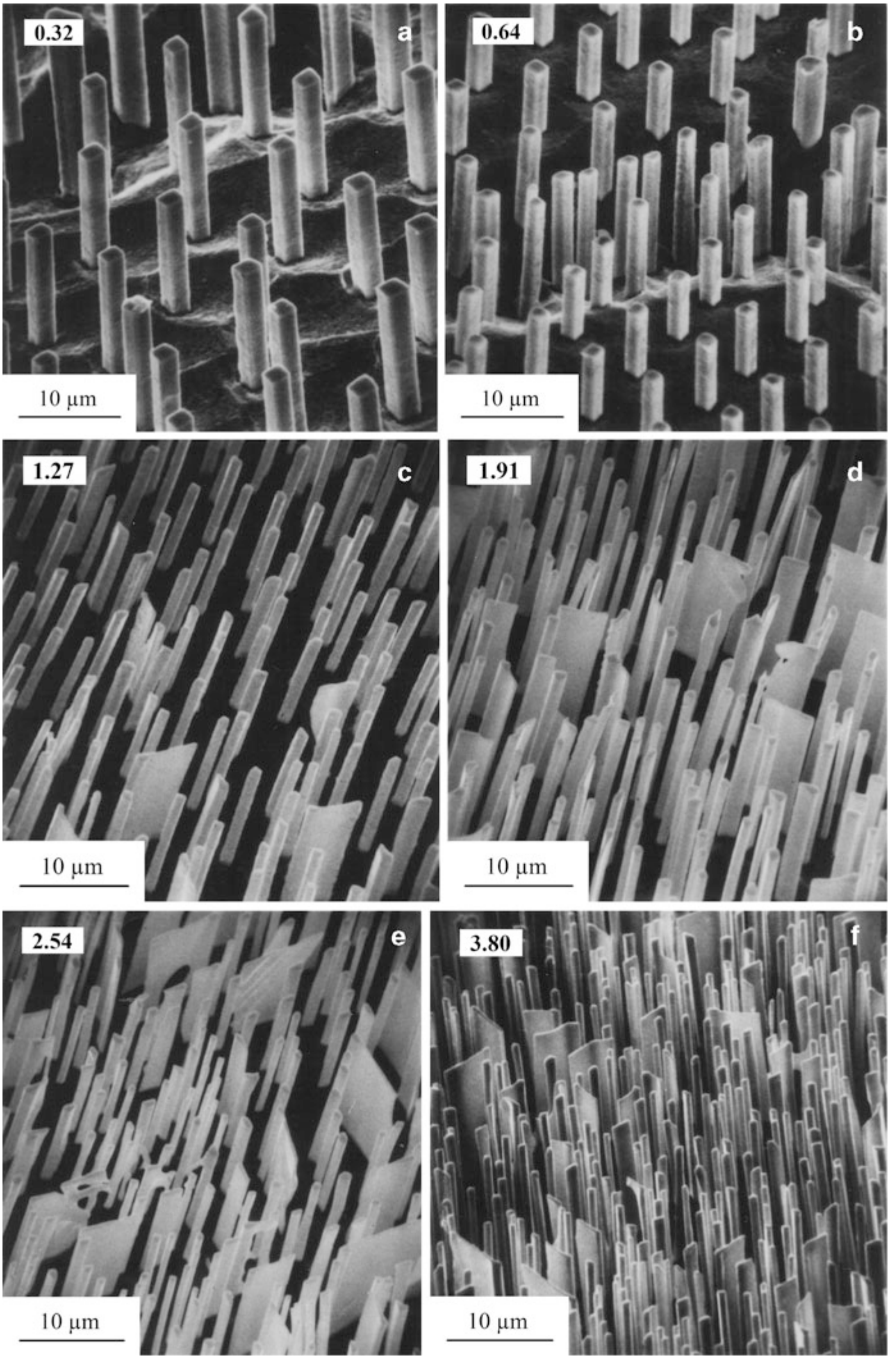

Fig. 6.9 Transverse sections of in situ composites obtained from a eutectic at different solidification rates indicated in *left-hand top* corners (cm/h). The nickel alloy matrix has been etched away to reveal the TaC fibers. [From Walter (1982), used with permission]

Table 6.2 Some important in situ composite systems

System	Carbide (vol. %)	T_E^a (°C)
Co–NbC	12	1,365
Co–TiC	16	1,360
Co–TaC	10	1,402
Ni–HfC	15–28	1,260
Ni–NbC	11	1,330
Ni–TiC	7.5	1,307

[a] T_E is the eutectic temperature

composition. An example of this is the addition of lithium to aluminum to improve the wettability in the alumina fiber/aluminum composite (Champion et al. 1978; Chawla 1989). However, in addition to wettability, there are other important factors such as chemical, mechanical, thermal, and structural ones that affect the nature of bonding between reinforcement and matrix. As it happens, these factors frequently overlap, and it may not always be possible to isolate these effects.

6.4.1 Major Discontinuities at Interfaces in MMCs

As we said earlier, at the interface a variety of discontinuities can occur. The important parameters that can show discontinuities in MMCs at a ceramic reinforcement/metal matrix interface are as follows:

- *Bonding*. A ceramic reinforcement will have an ionic or a mixed ionic/covalent bonding, while the metal matrix will have a metallic bonding.
- *Crystallography*. The crystal structure and the lattice parameter of the matrix and the reinforcement will be different.
- *Moduli*. In general, the elastic moduli of the matrix and the reinforcement will be different.
- *Chemical potential*. The matrix and the reinforcement will not be in thermodynamic equilibrium at the interface, i.e., there will be a driving force for a chemical reaction.
- *Coefficient of thermal expansion* (*CTE*). The matrix and the reinforcement will, in general, have different CTEs.

6.4.2 Interfacial Bonding in Metal Matrix Composites

Here we provide a summary of salient features of the interfacial region in some of the most important metal matrix composites.

6.4.2.1 Crystallographic Nature

In crystallographic terms, ceramic/metal interfaces in composites are, generally, incoherent, high-energy interfaces. Accordingly, they can act as very efficient vacancy sinks, provide rapid diffusion paths, segregation sites, sites of heterogeneous precipitation, and sites for precipitate free zones. Among the possible exceptions to this are the eutectic composites (Cline et al. 1971) and the XD™-type particulate composites (Mitra et al. 1993). In eutectic composites, X-ray and electron diffraction studies show preferred crystallographic growth directions, preferred orientation relationships between the phases, and low-index habit planes. Boundaries between in situ components are usually semicoherent, and the lattice mismatch across the interfaces can be accommodated by interface dislocations. Figure 6.10 shows a network of dislocations between the NiAl matrix and a chromium rod in a unidirectionally solidified NiAl–Cr eutectic (Cline et al. 1971).

6.4.2.2 Mechanical Bonding

Some bonding must exist between the ceramic reinforcement and the metal matrix for load transfer to occur from matrix to fiber. Two main categories of bonding are mechanical and chemical. Mechanical keying between two surfaces can lead to bonding. Hill et al. (1969) confirmed this experimentally for tungsten filaments in an aluminum matrix, while Chawla and Metzger (1978) observed mechanical

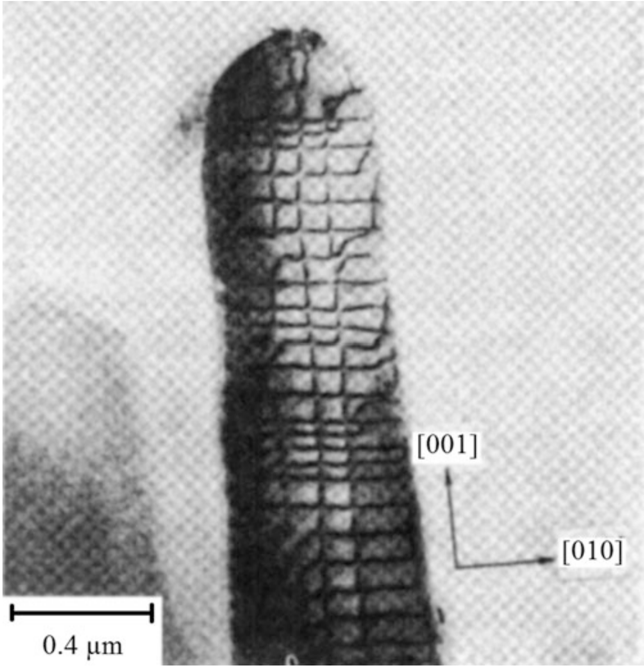

Fig. 6.10 A network of dislocations between the NiAl matrix and a chromium rod in a unidirectionally solidified NiAl–Cr eutectic. [Reprinted with permission from Acta Mater, 19, H.E. Cline et al. 1971, Pergamon Press Ltd.]

Fig. 6.11 The linear density of cracks in alumina as a function of strain in an alumina/aluminum composite for different degrees of interface roughness. The crack density continues to increase to larger strain values in the case of a rough interface (deeply etched pits) vis à vis a smooth or not very rough interface

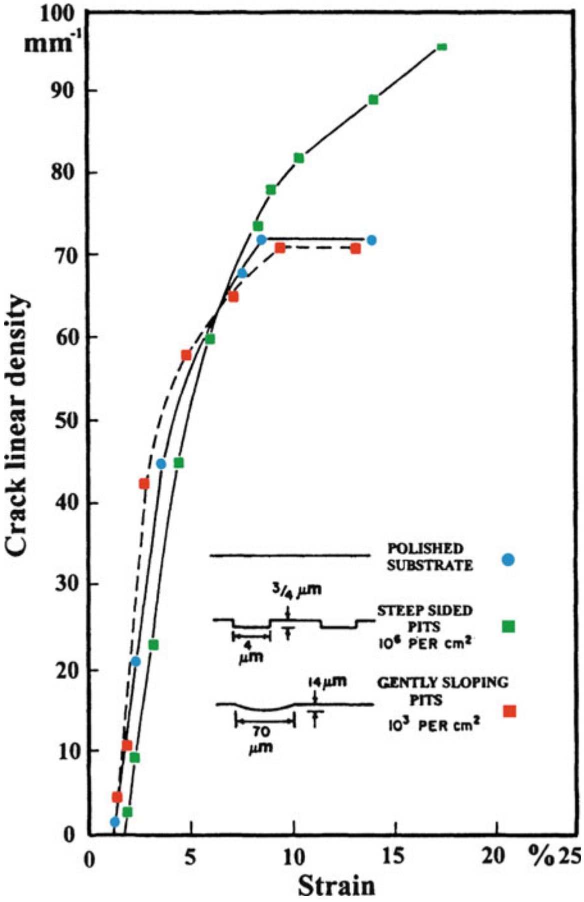

gripping effects at Al_2O_3/Al interfaces. The results of Chawla and Metzger (1978) are shown in Fig. 6.11 in the form of linear density of cracks (number of cracks per mm) in alumina as a function of strain in an alumina/aluminum composite for different degrees of interface roughness. The main message of this figure is that the crack density continues to increase to larger strain values in the case of a rough interface (deeply etched pits) vis à vis a smooth or not very rough interface, i.e., the rougher the interface, the stronger the mechanical bonding.

We can make an estimate of the radial stress, σ_r, at the fiber/matrix interface due to roughness induced gripping by using the following expression (Kerans and Parthasarathy 1991):

$$\sigma_r = \frac{-E_m E_f}{E_f(1+\nu_m) + E_m(1-\nu_f)}\left[\frac{A}{r}\right],$$

where E is the Young's modulus, ν is the Poisson's ratio, A is the amplitude of roughness, r is the radius of the fiber, and the subscripts m and f indicate matrix and fiber, respectively. For a given composite, the compressive radial stress increases with the roughness amplitude and decreases with the fiber radius. An important example of such an MMC, i.e., nonreacting components with purely a mechanical bond at the interface, is the filamentary superconducting composite consisting of niobium–titanium alloy filaments in a copper matrix.

6.4.2.3 Chemical Bonding

Ceramic/metal interfaces are generally formed at high temperatures. Diffusion and chemical reaction kinetics are faster at elevated temperatures. One needs to have knowledge of the chemical reaction products and, if possible, their properties. Molten iron, nickel, titanium, low alloy steels, austenitic and ferritic stainless steels, and nickel-based superalloys react with silicon-containing ceramics to form eutectics, with the reaction products being mainly metal silicides and carbides. It is thus imperative to understand the thermodynamics and kinetics of reactions in order to control processing and obtain optimum properties. We provide some examples.

Most metal matrix composite systems are nonequilibrium systems in the thermodynamic sense; that is, there exists a chemical potential gradient across the fiber/matrix interface. This means that given favorable kinetic conditions (which in practice means a high enough temperature or long enough time), diffusion and/or chemical reactions will occur between the components (see Fig. 4.4 in Chap. 4). Two common morphologies of reaction products at an interface in common metal matrix composites are as follows: (a) a reaction layer that covers the ceramic reinforcement more or less uniformly and (b) a discrete precipitation, particle or needle shaped, around the reinforcement. Type (a) reaction is controlled by diffusion of elements in the reaction layer. Typically, such a diffusional growth of the reaction layer scales as $x^2 \simeq Dt$, where x is the reaction layer thickness, t is the time, and D is the diffusion coefficient. Examples of systems showing such interfacial reactions include B/Al and SiC/Ti. Fujiwara et al. (1995) observed such a parabolic growth of the reaction zone in SCS-6 silicon carbide fiber/Ti-4.5Al-3V-2Fe-2Mo (wt.%) composites at three different temperatures. Figure 6.12 shows the reaction zone thickness squared (x^2) as a function of reaction time for three different

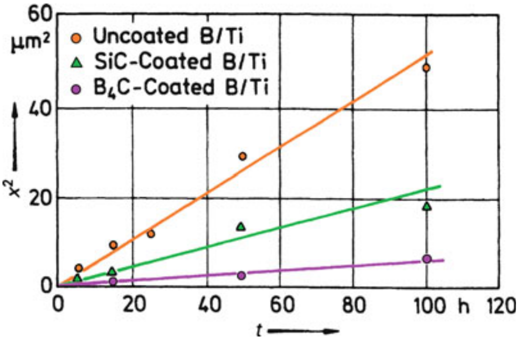

Fig. 6.12 Reaction zone thickness squared (x^2) as a function of reaction time for three different B/Ti composites. A B_4C carbide coating on the boron is most effective for the B/Ti system. [From Naslain et al. (1976), used with permission]

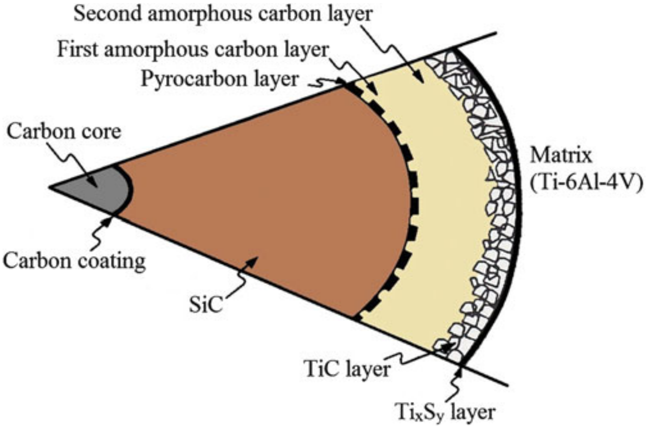

Fig. 6.13 Schematic of the interface region in silicon carbide fiber reinforced titanium matrix composites. [Adapted from Gabryel and McLeod (1991)]

boron fiber/titanium matrix composites. Note that the B_4C coating is more effective for the B/Ti system.

Silicon carbide fiber reinforced titanium matrix composites are attractive for some aerospace applications. Titanium and its alloys are very reactive in the liquid state; therefore, only solid state processing techniques such as diffusion bonding are used to make these composites (Partridge and Ward-Close 1993). In particular, a titanium alloy matrix containing SCS-6-type silicon carbide fiber can have a very complex interfacial chemistry and microstructure. A schematic of the interface region in these composites is shown in Fig. 6.13 (Gabryel and McLeod 1991). The pyrocarbon layer and the amorphous carbon layers are provided on the fiber surface, while the Ti silicides form during processing of the MMC.

Type (b) reaction involving precipitation at the interface is controlled by the nucleation process, followed by discrete precipitation at the reinforcement/matrix interface. Examples include alumina/magnesium, carbon/aluminum, and alumina–zirconia/aluminum. Figure 6.14 shows an example, a dark field TEM micrograph, of the reaction zone between alumina fiber and magnesium matrix. Also to be seen in this figure are the deformation twins in the matrix, the result of thermal stresses on cooling during liquid metal infiltration. Aluminum oxide can react with magnesium present in an aluminum alloy (Jones et al. 1993):

$$3\,\mathrm{Mg} + \mathrm{Al_2O_3} \leftrightarrow 3\,\mathrm{MgO} + 2\,\mathrm{Al}$$
$$3\,\mathrm{Mg} + 4\mathrm{Al_2O_3} \leftrightarrow 3\,\mathrm{MgOAl_2O_3} + 2\mathrm{Al}.$$

At high levels of Mg and low temperatures, MgO is expected to form, while the spinel forms at low levels of magnesium (Pfeifer et al. 1990).

A good example of obtaining a processing window by exploiting the kinetics of interfacial reaction between the fiber and matrix can be seen in the work of Isaacs

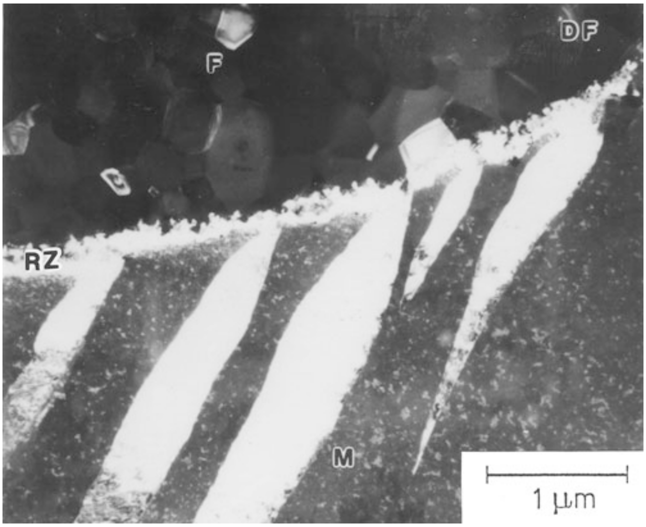

Fig. 6.14 A controlled amount of interfacial reaction at the Al_2O_3 fiber/Mg alloy matrix interface. *M, F*, and *RZ* denote matrix, fiber, and reaction zone, respectively. Dark field (DF) transmission electron micrograph

et al. (1991). These authors examined the interface structure in an aluminum matrix reinforced with an (alumina + zirconia) fiber. The composite made by pressure infiltration of the fibrous preform by liquid aluminum at 973 K (700°C), with a dwell time of 13 min, showed faceted $ZrAl_3$ platelets growing from the fiber into a matrix. However, they could suppress the kinetics of interfacial reaction by minimizing the high temperature exposure. No interfacial reaction product was observed when they processed the composite with the initial fibrous preform temperature below the melting point of aluminum and the solidification time less than 1 min.

Carbon fiber reacts with molten aluminum to form aluminum carbide, which is a very brittle compound and highly susceptible to corrosion in humid environments. Thus, it becomes imperative to use a barrier coating on carbon fibers before bringing them in contact with the molten aluminum. The carbon fibers are coated with a codeposition of Ti + B (presumably giving TiB_2). The starting materials for the coating process are: $TiCl_4$ (g), BCl_3 (g), and Zn (v); the possible reaction products are: TiB_2, $TiCl_2$, $TiCl_3$, and $ZnCl_3$. Any residual chloride in the coating is highly undesirable from a corrosion-resistance point of view.

In the case of carbon fibers in aluminum, poor wettability is a major problem. The wettability seems to improve somewhat when temperature increases above 1,000°C (Manning and Gurganus 1969; Rhee 1970), but it turns out that above 500°C a deleterious reaction occurs between the carbon fibers and the aluminum matrix, whereby Al_4C_3, a very brittle intermetallic compound, is known to form (Baker and Shipman 1972). Fiber surface coatings have also been tried. Such coatings do allow wetting by low-melting-point metals, but these coatings are

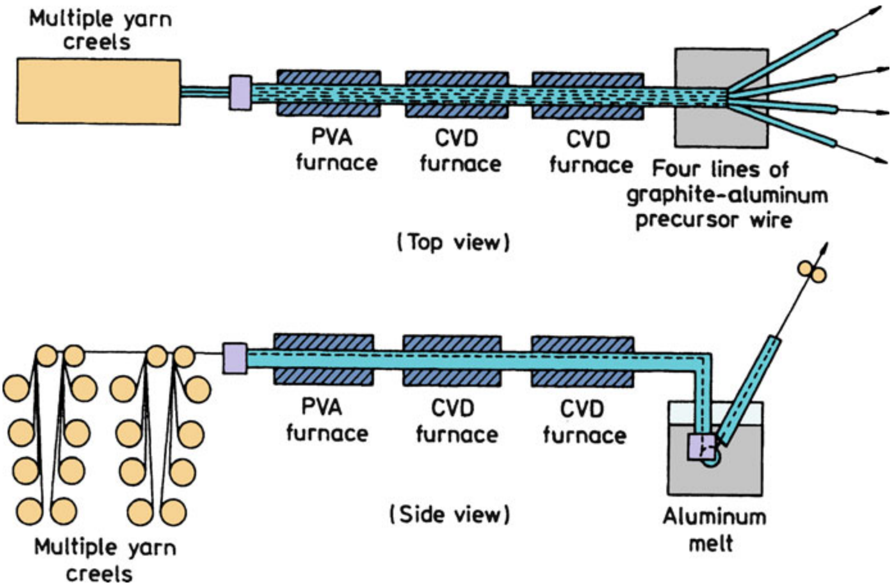

Fig. 6.15 Schematic of the Ti/B codeposition process for making carbon fiber/aluminum composites. [From Meyerer et al. (1978), used with permission]

also unstable in molten metals. Fiber degradation leading to reduced composite strength generally results. In the case of carbon fiber/aluminum composites, codeposition of titanium and boron onto carbon fibers before incorporating them into an aluminum matrix came to be established as a commercial method for carbon fiber surface treatment. Figure 6.15 shows a schematic of this process (Meyerer et al. 1978). Multiple yarn creels result in increased capacity over single yarn creels. The common size on carbon fibers such as polyvinyl alcohol (PVA) (meant for polymeric matrices) is removed in a furnace, designated as a PVA furnace in Fig. 6.15.

The first CVD furnace in Fig. 6.15 is a precoat furnace for cleaning and activating the carbon yarn surface. The Ti/B coating is deposited in the second CVD furnace, followed by drawing through a molten aluminum bath.

Warren and Andersson (1984) have reviewed the thermodynamics of chemical equilibria between SiC and some common metals. They divide these systems into *reactive* and *stable* types. In reactive systems, SiC reacts with the metal to form silicides and/or carbides and carbon. No two-phase field exists in the ternary phase diagram showing SiC and the metal in equilibrium. For example, with nickel and titanium, the following reactions are possible:

$$\mathrm{SiC} + \mathrm{Ni} \rightarrow \mathrm{Ni}_x\mathrm{Si}_y + \mathrm{C}$$

$$\mathrm{SiC} + \mathrm{Ti} \rightarrow \mathrm{Ti}_x\mathrm{Si}_y + \mathrm{TiC}\ \ (\text{low SiC fractions}).$$

Such reactions are thermodynamically possible between SiC and nickel or titanium, but in practice, reaction kinetics determine the usefulness of the composite. In stable systems, SiC and a metallic matrix alloy can coexist thermodynamically, that is, a two-phase field exists. Examples are SiC fibers in alloys of aluminum, gold, silver, copper, magnesium, lead, tin, and zinc. This does not imply that SiC will not be attacked. In fact, a fraction of SiC fibers in contact with molten aluminum can dissolve and react to give Al_4C_3:

$$\mathrm{SiC} + \mathrm{Al} \rightarrow \mathrm{SiC} + (\mathrm{Si}) + \mathrm{Al_4C_3}.$$

This reaction can happen because the section SiC-Al lies in a three-phase field. Such reactions can be avoided by prior alloying of aluminum with silicon.

The interface product(s) formed because of a reaction will generally have characteristics different from those of either component. It should be pointed out, however, that at times, some controlled amount of reaction at the interface, such as that shown in Fig. 6.14, may be desirable for obtaining strong bonding between the fiber and the matrix, but, too thick an interaction zone will adversely affect the composite properties.

Silicon carbide particle reinforced aluminum composites have been investigated extensively. An important processing technique for these MMCs involves liquid metal infiltration of a particulate preform. In a silicon-free aluminum alloy matrix, silicon carbide and molten aluminum can react as follows:

$$4\,\mathrm{Al}(l) + 3\mathrm{SiC}(s) \leftrightarrow \mathrm{Al_4C_3}(s) + 3\mathrm{Si}(s).$$

The forward reaction will add silicon to the matrix. As the silicon level increases in the molten matrix, the melting point of the alloy decreases with time. The reaction can be made to go leftward by using high silicon alloys. This, of course, restricts the choice of Al alloys for liquid route processing. Table 6.3 gives a summary of interfacial reactions in some important MMCs.

In general, ceramic reinforcements (fibers, whiskers, or particles) have a coefficient of thermal expansion smaller than that of most metallic matrices. This means that when the composite is subjected to a temperature change, thermal stresses

Table 6.3 Interfacial reaction products in some important MMCs

Reinforcement	Matrix	Reaction product(s)
SiC	Ti alloy	TiC, Ti_5Si_3
	Al alloy	Al_4C_3
Al_2O_3	Mg alloy	MgO, $MgAl_2O_4$ (spinel)
C	Al alloy	Al_4C_3
B	Al alloy	AlB_2
Al_2O_3 + ZrO_z	Al alloy	$ZrAl_3$
W	Cu	None
C	Cu	None
Al_2O_3	Al	None

will be generated in both of the components. This observation is true for all composites—polymer, metal, and ceramic matrix composites. What is unique of metal matrix composites is the ability of a metal matrix to undergo plastic deformation in response to the thermal stresses generated and thus alleviate them. Chawla and Metzger (1972), working with a single crystal copper matrix containing large diameter tungsten fibers, showed the importance of thermal stresses in MMCs. Specifically, they employed a dislocation etch-pitting technique to delineate dislocations in single-crystal copper matrix and showed that near the fiber the dislocation density was much higher in the matrix than the dislocation density far away from the fiber. The situation in the as-cast composite can be depicted as shown schematically in Fig. 6.16, where a primary plane section of the composite is shown having a hard zone (high dislocation density) around each fiber and a soft zone (low dislocation density) away from the fiber (Chawla 1975). The enhanced dislocation density in the copper matrix near the fiber arises because of the plastic deformation in response to the thermal stresses generated by the thermal mismatch between the fiber and the matrix. The intensity of the gradient in dislocation density will depend on the inter-fiber spacing. The dislocation density gradient will decrease with a decrease in the interfiber spacing. The existence of a plastically deformed zone containing high dislocation density in the metallic matrix in the vicinity of the reinforcement has since been confirmed by transmission electron microscopy by a number of researchers, both in fibrous and particulate metal matrix composites (Arsenault and Fisher 1983; Rack 1987; Christman and Suresh 1988). Such high dislocation density in the matrix can alter the precipitation behavior, and, consequently, the aging behavior in MMCs in those composites that have a precipitation hardenable alloy matrix (see Sect. 6.5).

We mentioned the roughness induced radial compression stress at the fiber/matrix interface in Sect. 6.4.2. As discussed earlier, the thermal mismatch between the components can lead to thermal residual stresses. Specifically, a radial stress component will be introduced which can be positive or negative. To obtain the net radial stress at the fiber/matrix interface, one should add the stresses algebraically from the two sources, viz., the contribution due to thermal mismatch between the reinforcement and the matrix and the stress arising due to the roughness induced gripping, as mentioned previously. A combined expression for the radial stress from these two sources can be written as (Kerans and Parthasarathy 1991)

$$\sigma_{\mathrm{r}} = \frac{-qE_{\mathrm{m}}E_{\mathrm{f}}}{E_{\mathrm{f}}(1+\nu_{\mathrm{m}}) + E_{\mathrm{m}}(1-\nu_{\mathrm{f}})}\left[\Delta\alpha\Delta T + \frac{A}{r}\right].$$

where q is an adjustable parameter (equal to 1 for an infinite matrix), E is the Young's modulus, ν is the Poisson's ratio, ΔT is the temperature change, $\Delta\alpha$ is the thermal mismatch between the fiber and the matrix $= (\alpha_{\mathrm{m}} - \alpha_{\mathrm{f}})$, A is the amplitude of roughness, r is the radius of the fiber, and the subscripts m and f refer to matrix and fiber, respectively. Thus, in the absence of chemical bonding, one can control the degree of interfacial bonding by controlling the degree of interfacial roughness, the thermal mismatch between the matrix and the reinforcement, and the amplitude of temperature change.

Metal matrix composites with reinforcement in the form of a short fiber, whisker, or particle (also called *discontinuously reinforced MMCs*), especially aluminum matrix composites can be subjected to conventional metalworking processes (e.g., rolling, forging, extrusion, machining, and swaging). Figure 6.17a shows a perspective montage (SEM) of a rolled plate of SiC (20 v/o)/2124 Al. The rolling direction is perpendicular to the original extrusion direction. The very small particles in Fig. 6.17a are the precipitates in the matrix after aging, while the large irregular particles are probably (Fe, Mn) Al_6. The distribution of SiC whiskers in the aluminum matrix, as seen in a transmission electron microscope, is shown in Fig. 6.17b, while a close-up of the whisker/matrix interface region is shown in Fig. 6.17c. Note the waviness of the interface. Fu et al. (1986) examined the interface chemistry and crystallography of C/Al and SiC_w/Al MMCs in the TEM. They observed an oxide at some of the SiC/Al interfaces. Figure 6.18a, b shows the TEM bright and dark field micrographs of the interface region of 20 v/o SiC_w/Al. The crystalline γ-Al_2O_3 phase is about 30 nm. It was, however, not uniformly present at every interface. In C/Al composites, both fine-grained γ-Al_2O_3 and coarse-grained Al_4C_3 were found at the interfaces. On heat treating, some of the Al_4C_3 grew into and along the porous sites at the carbon fiber surface.

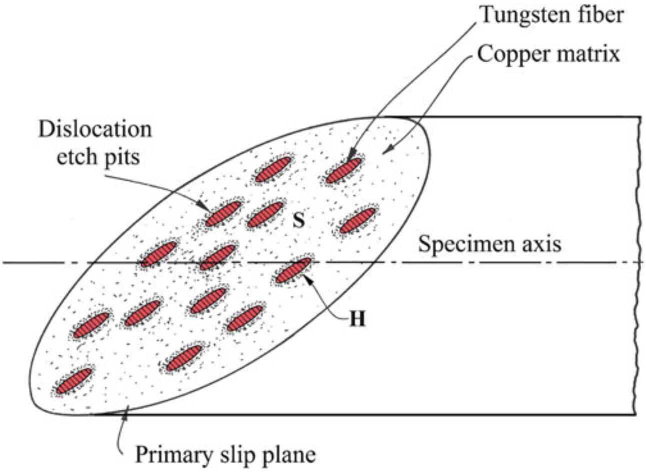

Fig. 6.16 A primary plane section of a metal matrix composite is shown as having a hard zone (high dislocation density) around each fiber and a soft zone (low dislocation density) away from the fiber

6.5 Properties

We describe some of the important mechanical and physical properties of metal matrix composites in this section.

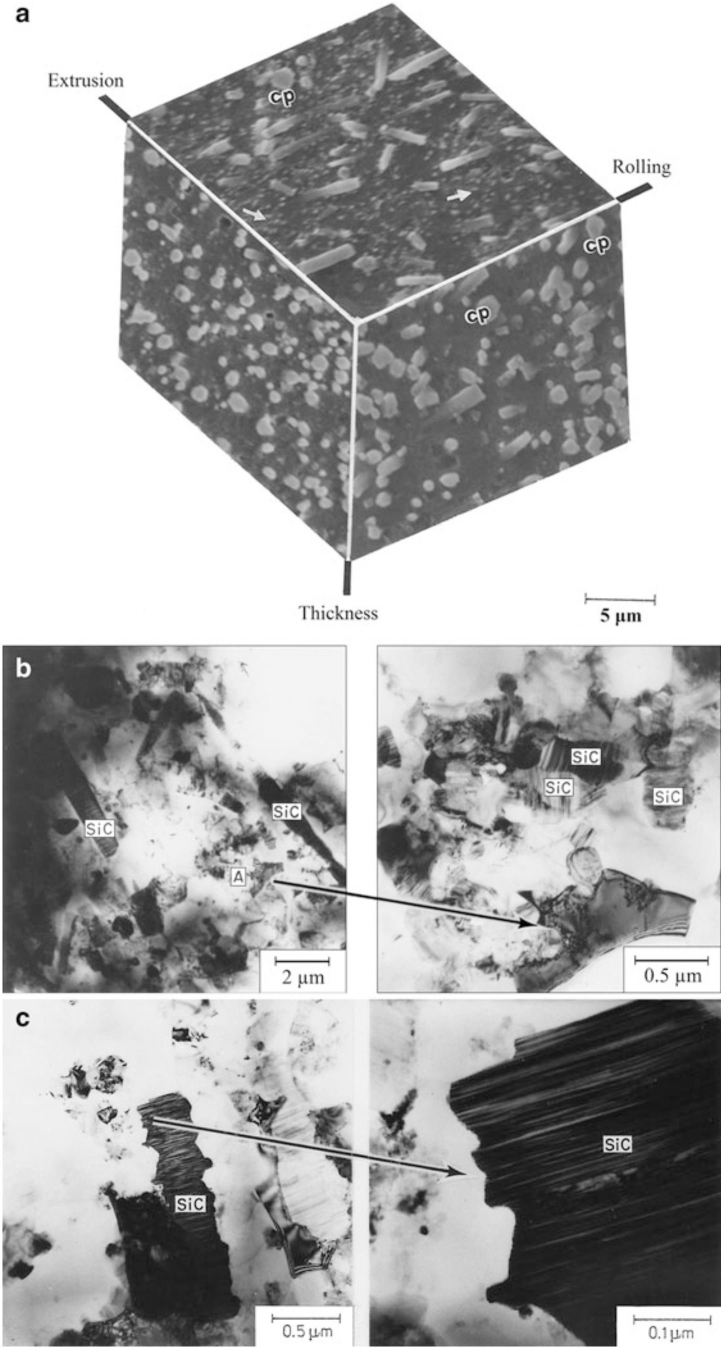

Fig. 6.17 (**a**) A perspective montage of a SiC/Al composite. The smallest particles (indicated by *arrows* on the *top face*) are precipitates from the matrix as a result of aging. Silicon carbide whiskers are

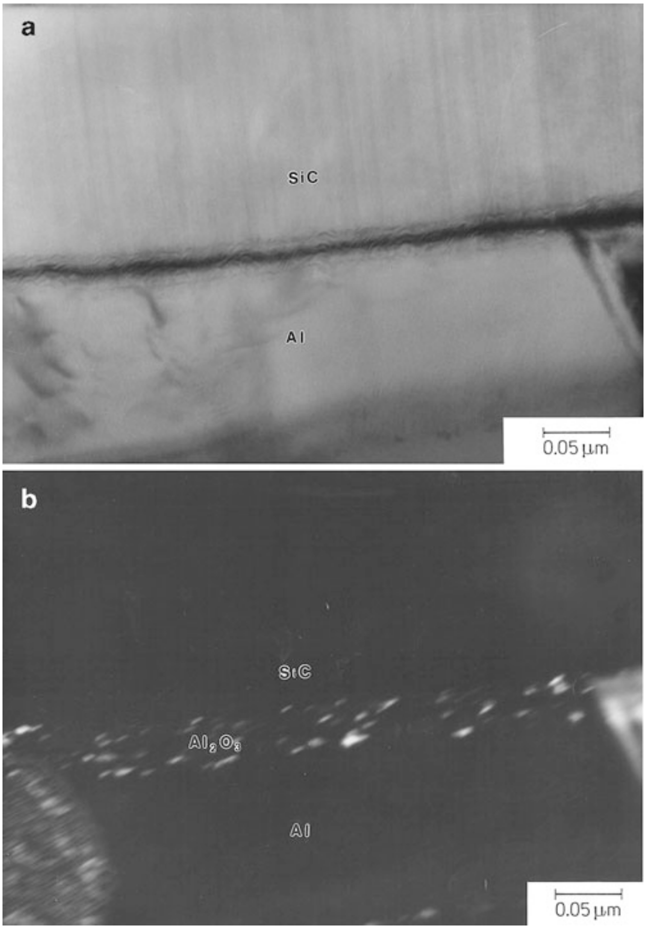

Fig. 6.18 Interface in SiC_w/Al composite: (**a**) bright field TEM, (**b**) dark field TEM showing the presence of $A1_2O_3$ at the interface. [From Fu et al. (1986), ©ASTM, reprinted with permission]

6.5.1 Modulus

Unidirectionally reinforced continuous fiber reinforced metal matrix composites show a linear increase in the longitudinal Young's modulus of the composite as a

Fig. 6.17 (continued) theintermediate particles, both long and narrow and equiaxial ones having a diameter similar to the width of the long, narrow ones. The large irregular particles are (Fe, Mn) Al_6-type constituent particles (some of these are marked cp). The liquid-phase hot-pressed billet was first extruded in the extrusion direction, forged along the thickness direction, and finally rolled along the rolling direction. (Courtesy of D.R. Williams and M.E. Fine.) (**b**) Distribution of SiC_w in an aluminum matrix (TEM). (**c**) A higher magnification of the whisker/matrix interface (TEM). [Courtesy of J.G. Greggi and P.K. Liaw] function of the fiber volume fraction. Figure 6.19 shows an example of modulus and strength increase as a function of fiber volume fraction for alumina fiber reinforced aluminum–lithium alloy matrix (Champion et al. 1978). The increase in the longitudinal Young's modulus is in agreement with the rule-of-mixtures value, while the modulus increase in a direction transverse to the fibers is very low. Particle reinforcement also results in an increase in the modulus of the composite; the increase, however, is much less than that predicted by the rule-of-mixtures. This is understandable inasmuch as the rule-of-mixtures is valid only for continuous fiber reinforcement. Figure 6.20 shows schematically increase in Young's modulus

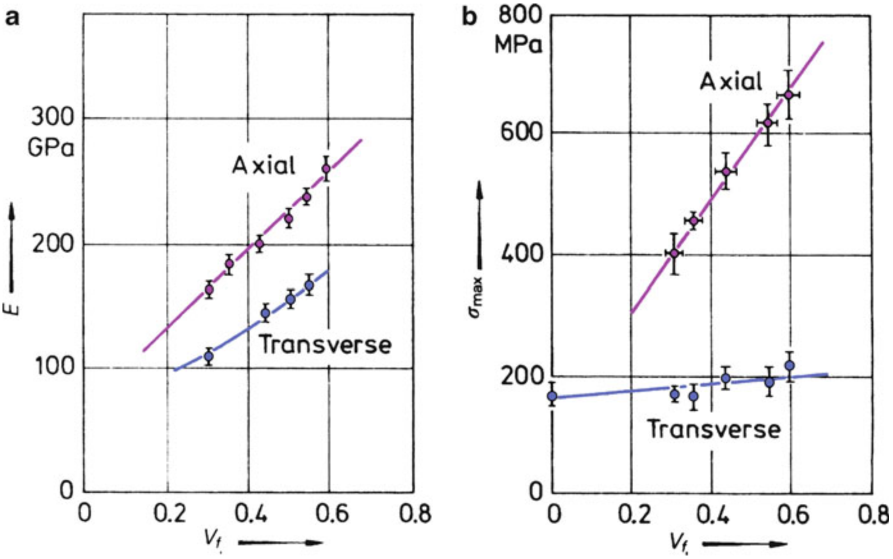

Fig. 6.19 Properties of Al_2O_3/Al–Li composites as a function of fiber volume fraction (V_f): (**a**) axial and transverse Young's modulus vs. fiber volume fraction, (**b**) axial and transverse ultimate tensile strength vs. fiber volume fraction. [From Champion et al. (1978), used with permission]

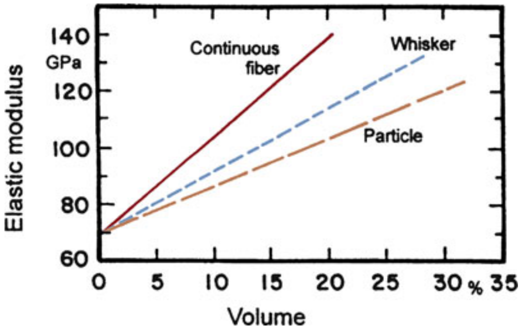

Fig. 6.20 Increase in Young's modulus of an MMC as a function of reinforcement volume fraction for continuous fiber, whisker, or particle reinforcement

of an MMC as a function of reinforcement volume fraction for different forms of reinforcement viz., continuous fiber, whisker, or particle. Note the loss of reinforcement efficiency as one goes from continuous fiber to particle. Metal matrix particulate composites, such as SiC particle reinforced aluminum can offer a 50–100% increase in modulus over that of unreinforced aluminum, i.e., a modulus equivalent to that of titanium but density about 33% less. Also, unlike the fiber reinforced composites, the stiffness enhancement in particulate composites is reasonably isotropic.

6.5.2 *Strength*

Prediction of strength of an MMC is more complicated than the prediction of modulus. This is so because there can be direct and indirect strengthening. The direct strengthening considers the contribution of fiber and the metal matrix without taking into account and strength contribution stemming from any microstructural changes in the metal matrix. The direct strengthening is described as follows. Consider an aligned fiber reinforced metal matrix composite under a load P_c in the direction of the fibers. This load is distributed between the fiber and the matrix. Thus,

$$P_c = P_m V_m + P_f V_f,$$

where P_m and P_f are the loads on the matrix and the fiber, and V_m and V_f are the volume fractions of the matrix and the fiber, respectively. This equation can be converted to the following rule-of-mixtures (we discuss this in more detail in Chap. 10) relationship under conditions of isostrain (i.e., the strain in the fiber, matrix, and composite is the same):

$$\sigma_c = \sigma_f V_f + \sigma_m V_m,$$

where σ is the stress, V is the volume fraction, and the subscripts c, f, and m denote the composite, fiber, and matrix, respectively. This equation, commonly referred to as the *Rule-of-Mixtures*, says that the strength of the composite is a volume-weighted average of the strengths of the fiber and the matrix.

On the face of it, there is nothing wrong with rule-of-mixtures as written above for strength. The problem is that one needs the in situ values of σ_f and σ_m. If the fiber remains essentially elastic up to the point of fracture, then σ_f, the fiber strength in the composite, is the same as that determined in an isolated test of the fiber. This is particularly true of ceramic fibers. The same, however, cannot be said for the metallic matrix. The matrix strength in the composite (the in situ strength) will, in

Table 6.4 Representative properties of some continuous fiber reinforced MMCs

Composite and direction	Fiber volume fraction (%)	Density (g/cm^3)	σ_{max} (MPa)	E (GPa)
B/Al				
0°	50	2.65	1,500	210
90°	50	2.65	140	150
SiC/Al				
0°	50	2.84	250	310
90°	50	2.84	105	–
SiC/Ti-6A1-4V				
0°	35	3.86	1,750	300
90°	35	3.86	410	–
Al_2O_3/Al–Li				
0°	60	3.45	690	262
90°	60	3.45	172–207	152
C(Thornel 50)/Mg alloy	38	1.8	510	–
C/Al	30	2.45	690	160

all likelihood, not be the same as that determined from a test of an unreinforced matrix sample in isolation. This is because the metal matrix can suffer several microstructural alterations during processing and, consequently, changes in its mechanical properties. This is what is called indirect strengthening. In view of the fact that, in general, ceramic reinforcements have a coefficient of thermal expansion smaller than that of most metallic matrices, thermal stresses will be generated in the two components, the fiber and the matrix. A series of events can take place in response to the thermal stresses (Chawla and Metzger 1972; Chawla 1973a, b, 1974):

1. Plastic deformation of the ductile metal matrix (slip, twinning, cavitation, grain boundary sliding, and/or migration).
2. Cracking and failure of the brittle fiber.
3. An adverse reaction at the interface.
4. Failure of the fiber/matrix interface.

In particular, plastic deformation (item #1 above) can result in an increased dislocation density in the metal matrix because of thermal stresses. Item 3 can also affect the strength depending on the nature and extent of the reaction product. We will discuss the subject of thermal stresses in Chap. 10. A discussion of the effect of thermal stresses on the strength properties of composites will be presented in Chap. 12. A summary of typical properties of long or continuous fiber reinforced MMCs is given in Table 6.4.

The indirect strengthening appears to be more important in particle reinforced composites. Arsenault and Shi (1986) and Shi and Arsenault (1991, 1993) analyzed various contributing factors in particulate MMCs, in the absence of a shear lag strengthening mechanism, which would be more effective in the case of long fibrous reinforcement. They enumerated the following indirect strengthening mechanisms in particulate MMCs:

- Orowan strengthening, which is given by Gb/l, where G is the shear modulus of the matrix, b is the Burgers vector of the matrix, and l is the particle spacing.
- Grain and substructure strengthening in the metal matrix, following a Hall–Petch-typerelationship, i.e., strength varying as $d^{-1/2}$, where d is the grain or subgrain size in the matrix. The Hall–Petch slope k for Al is in the range of 0.1–0.15 MPa $\sqrt{}\mathrm{m}^2$, i.e., it is very low, while for steels, k is very high. Thus, a grain diameter $d < 10$ μm will give significant strengthening, while $d < 1$ μm can give very good strengthening.
- Quench strengthening with thermal strain in the matrix given by $e_\mathrm{m} = \Delta\alpha\Delta T$. According to the model of Arsenault and Shi (1986), dislocation punching occurs in the matrix due to thermal mismatch. The dislocation density resulting from the coefficient of thermal expansion mismatch is

  $$\rho_\mathrm{CTE} = (AeV_\mathrm{p})/b(1 - V_\mathrm{p})d,$$

  where A is a geometric constant, e is the thermal misfit strain, A is the particle area, b is the Burgers vector, and V_p is the particle volume fraction.

  The corresponding stress is given by

  $$\sigma_\mathrm{q} = \alpha Gb(\rho_\mathrm{CTE})^{1/2},$$

  where α is a constant. This contribution to strength can be significant.
- Work hardening of the matrix. Particles affect the matrix work hardening rate.

In powder metallurgy processed composites, fine oxide from the SiC particle's surface can enter the matrix. The contribution of grain boundary strengthening is given by

$$\sigma_\mathrm{gb} = kd^{-1/2}.$$

Grain boundary strengthening can be high in spray cast and powder metallurgy processed composites.

It is thus complicated to predict the strength of a particulate MMC. An analysis (Nardone and Prewo 1986) that takes into account tensile loading at the particle ends gives the following expression for the yield strength of a particulate composite

$$\sigma_\mathrm{yc} = \sigma_\mathrm{ym}[1 + (L + t)/4L]V_\mathrm{p} + \sigma_\mathrm{ym}(1 - V_\mathrm{p}),$$

where σ_ym is the yield stress of the unreinforced matrix, V_p is the particle volume fraction, L is the length of the particle perpendicular to the applied load and t is the length of the particle parallel to the loading direction (see also Chap. 10).

6.5.2.1 Effect of Thermal Stresses

It is important to realize is that the matrix in composites is not merely a kind of glue or cement to hold the reinforcement in place [Chawla 1985]. The characteristics of the matrix, as modified by the introduction of fibers, must be evaluated and exploited to obtain an optimum set of properties of the composite. The nature of the fibers or particles, fiber or particle diameter, and distribution, as well as conventional solidification parameters, all influence the final matrix microstructure. Porosity is one of the major defects in cast MMCs, owing to the shrinkage of the metallic matrix during solidification. At high fiber volume fractions, the flow of interdendritic liquid becomes difficult, and large scale movement of semisolid metal may not be possible. More importantly, the microstructure of the metallic matrix in a fiber composite can differ significantly from that of the unreinforced metal. Mention has been made of higher dislocation density in the metal matrix because of plastic deformation originating in thermal stresses (Chawla and Metzger 1972). Mortensen et al. (1986) showed that the presence of fibers influences the solidification of the matrix alloy. Figure 6.21a shows a cross section of an SCS-2 silicon carbide fiber/Al-4.5% Cu matrix. Note the normal dendritic cast structure in the unreinforced region, whereas in the reinforced region the dendritic morphology is controlled by the fiber distribution. Figure 6.21b shows the same system at a higher magnification. The second phase (θ) appears preferentially at the fiber/matrix interface or in the narrow interfiber spaces. Kohyama et al. (1985) observed that shrinkage cavities present in the matrix in SiC/Al composites were the predominant crack-initiation sites. They also observed a wavy interface structure between SiC and the aluminum matrix, indicating some mechanical bonding in addition to any chemical and physical bonding. In the system SiC/Mg (AZ19C), they observed a magnesium-rich interfacial layer that acted as the fracture-initiating site.

Frequently the metal matrix alloy used in an MMC has precipitation hardening characteristics, i.e., such an alloy can be hardened by a suitable heat treatment, called *aging treatment*. It has been shown by many researchers (Esmaeili et al. Dunand and Mortensen 1991a, b; Dutta et al. 1988; Dutta and Bourell 1988; 1990; Chawla et al. 1991; Nieh and Karlak 1984; Parrini and Schaler 1994) that the microstructure of the metallic matrix is modified by the presence of ceramic reinforcement and consequently the standard aging treatment for, say, an unreinforced aluminum alloy will not be valid (see Suresh and Chawla (1993) for a review of this topic). The reinforcements (fiber or particle), such as SiC, B_4C, Al_2O_3, are unaffected by the aging process. These reinforcements, however, can affect the precipitation behavior of the matrix quite significantly. In particular, as we pointed out earlier, a higher dislocation density in the matrix metal or alloy than that in the unreinforced metal or alloy is produced. The higher dislocation density in the matrix has its origin in the thermal mismatch ($\Delta\alpha$) between the reinforcement and the metallic matrix. This thermal mismatch can be quite large, for example, in the case of SiC and aluminum, it has a high value of 21×10^{-6}/K. The precipitate-hardenable aluminum alloy matrix has a more important role to play in these composites than a nonhardenable matrix material. A considerable strength increment results due to the age-hardening treatments. One would

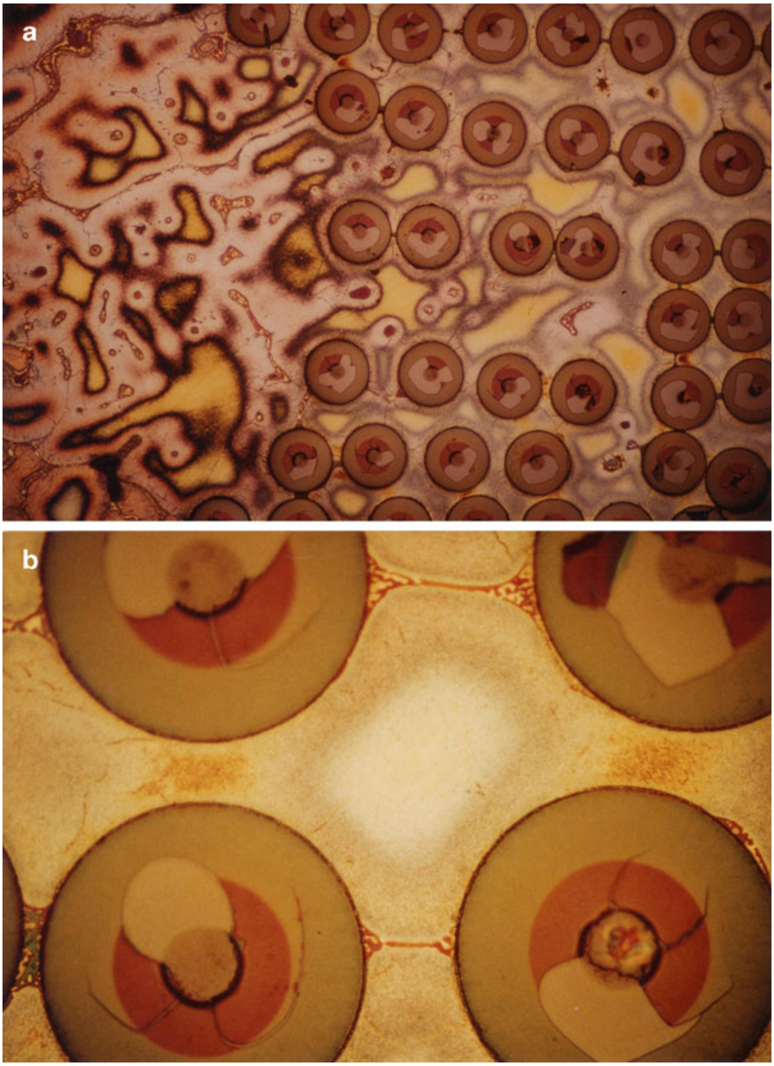

Fig. 6.21 Transverse section of an SCS-2 SiC fiber in an Al-4.5 % Cu matrix. (**a**) Note the difference in the dendritic structure of the unreinforced and the fiber-rich regions of the matrix. (**b**) the second phase appears preferentially at the fiber/matrix interface or in the narrow interfiber region. The fiber diameter is 142 μm in both (**a**) and (**b**). [Reprinted with permission from J Metals 37(6):45, 47, and 48, a publication of the Metallurgical Society, Warrendale, Pennsylvania]

expect that the high dislocation density will also affect the precipitation kinetics in a precipitation-hardenable matrix such as 2XXX series aluminum alloy. Indeed, faster precipitation kinetics have been observed in the matrix than in the bulk unreinforced alloy. This has very important practical implications. One may not use the standard heat treatments commonly available in various handbooks, say, for monolithic aluminum alloys for the same alloy used as a matrix in an MMC.

6.5.2.2 Properties of In Situ Composites

We mentioned earlier the class of MMCs called in situ composites. An important example of such a system is a composite made by directional solidification of a eutectic alloy. The strength, σ, of such an in situ metal matrix composite is given by a relationship similar to the Hall–Petch relationship used for grain boundary strengthening of metals (Meyers and Chawla 1984):

$$\sigma = \sigma_o + k\lambda^{-1/2},$$

where σ_o is a friction stress term, k is a material constant, and λ is the spacing between rods or lamellae. It turns out that one can vary the interfiber spacing, λ, rather easily by controlling the solidification rate, R, because

$$\lambda^2 R = \text{constant}.$$

van Suchtelen (1972) has classified eutectic or in situ composites into two broad categories from an electronic property viewpoint:

1. *Combination-type properties*. This can be further subdivided into (a) sum type and (b) product type. In *sum type*, properties of the constituent phases contribute proportionately to their amount. Examples are heat conduction, density, and elastic modulus. In the *product type*, the physical output of one phase serves as input for the other phase: for example, conversion of a magnetic signal into an electrical signal in a eutectic composite consisting of a magnetostrictive phase and a piezoelectric phase.
2. *Morphology-dependent properties*. In this case, the properties depend on the periodicity and anisotropy of the microstructure, the shape and size of the phases, and the amount of interface area between the phases. A good example is InSb–NiSb, which is a quasibinary system with a eutectic at 1.8% NiSb. Unidirectional solidification of a eutectic melt at a growth rate of 2 cm/h results in an aligned composite consisting of an InSb semiconducting matrix containing long hexagonal fibers of the NiSb phase. The magnetoresistance of the InSb–NiSb composite becomes extremely large if the directions of the metallic fibers, the electric current, and the magnetic field are mutually perpendicular. This characteristic has been exploited in making contactless control devices; a practical example is described in Sect. 6.6.

6.5.2.3 Properties of Particulate Composites

Tensile stress–strain curves of SiC_p/Al composites are shown in Fig. 6.22 (Chawla et al. 1998). Figure 6.22a shows the true stress–true strain curves for one particle size (6 μm) but different volume fractions of the SiC particles. As the particle volume fraction increases, the strength of the composite increases but the ductility decreases. Figure 6.22b shows the true stress–true strain curves for different particle sizes but for a fixed volume fraction (20% by volume). The strength increases as the particle size decreases.

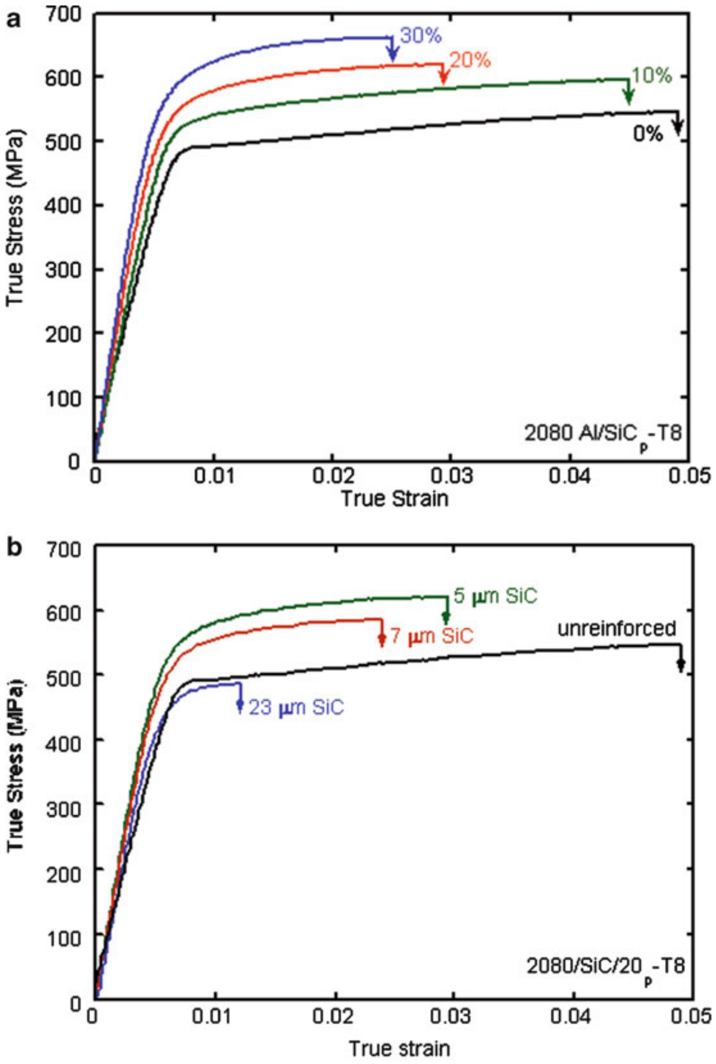

Fig. 6.22 (**a**) True stress–true strain curves for different volume fractions of the SiC particles in aluminum matrix (6 μm). As the particle volume fraction increases, the strength of the composite increases but the ductility decreases. (**b**) True stress–true strain curves for different particle sizes but for a fixed volume fraction (20 % by volume). The strength increases as the particle size decreases. [Courtesy of N. Chawla]

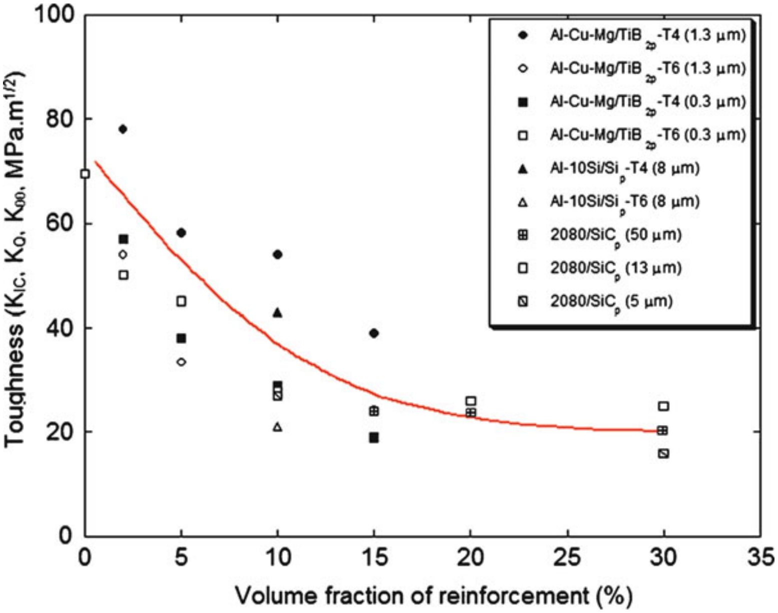

Fig. 6.23 Toughness in several particulate composite systems as a function of reinforcement volume fraction. All the composites show a decrease in toughness with increasing volume fraction of reinforcement [after Manoharan et al. 1993; Hunt et al. 1993, and Beck Tan et al. 1994]

Toughness can be regarded as a measure of energy absorbed in the process of fracture, or more specifically as the resistance to crack propagation, K_{Ic}. The toughness of MMCs depends on the following factors:

- matrix alloy composition and microstructure
- reinforcement type, size, and orientation
- processing, insofar as it affects microstructural variables (e.g., distribution of reinforcement, porosity, segregation, and so on)

For a given V_{f}, the larger the diameter of the fiber, the tougher the composite. This is because the larger the fiber diameter, for a given fiber volume fraction, the larger the amount of tough, metallic matrix in the interfiber region that can undergo plastic deformation and thus contribute to the toughness.

Unidirectional fiber reinforcement can lead to easy crack initiation and easy propagation vis à vis the unreinforced alloy matrix. Braiding of fibers can make the crack propagation toughness increase tremendously due to extensive matrix deformation, fiber bundle debonding, and pullout (Majidi and Chou 1987). The general range of K_{Ic} values for particle reinforced aluminum-type MMCs is between 15 and 30 MPa m$^{1/2}$, while short fiber- or whisker-reinforced MMCs have $\simeq$5–10 MPa m$^{1/2}$.

The fracture toughness of particle reinforced MMCs is controlled by: (a) volume fraction of reinforcement, (b) interparticle spacing and strength of particles, (c) spatial distribution of particles (i.e., particle clustering), and (d) matrix microstructure (as controlled by heat-treatment in age-hardenable alloys). Figure 6.23 shows toughness in several particulate composite systems as a function of reinforcement volume fraction. All the composites show a decrease in toughness with increasing volume fraction of reinforcement. The toughness appears to reach a "plateau" at volume fraction of 20% and above. The decrease in toughness is attributed to an increase in stress triaxiality with increasing volume fraction of particles.

Among the explanations for low toughness values of the composites are the following variables: the type of intermetallic particles, inhomogeneous internal stress, and particle or whisker distribution. Improvements in fracture toughness of SiC_w/Al composites and K_{Ic} values levels equivalent to those of 7075 A1(T6) have been obtaind by using a cleaner matrix powder, better mixing, and increased mechanical working during fabrication (McDanels 1985). McDanels' work also reinforces the idea that the metallic matrix is not merely a medium to hold the fibers together. The type of aluminum matrix used in 20 v/o SiC_w/Al composites was the most important factor affecting yield strength and ultimate tensile strength of these composites (McDanels 1985). Higher-strength aluminum alloys showed higher strengths but lower ductilities. Composites with 6061 Al matrix showed good strength and higher fracture strain.

6.5.3 Thermal Characteristics

In general, ceramic reinforcements (fibers, whiskers, or particles) have a coefficient of thermal expansion smaller than that of most metallic matrices. This means that when the composite is subjected to a temperature change (deliberate or inadvertent), thermal stresses will be generated in both the components because of the constraint imposed by the interfacial bonding.

Chawla and Metzger (1972), working with a single crystal copper matrix containing large-diameter tungsten fibers, showed the importance of thermal stresses in MMCs. Specifically, they employed a dislocation etch-pitting technique to delineate dislocations in a single crystal copper matrix. This system has the advantage of showing pure fiber reinforcement, i.e., no interfacial reaction, no grain boundaries in the matrix, etc. They showed that, in their low fiber volume fraction composites, near the fiber the dislocation density was much higher in the matrix than the dislocation density far away from the fiber. The situation in the as-cast composite can be depicted as was shown schematically in Fig. 6.15, where a primary plane section of the composite is shown having a hard zone (high dislocation density) around each fiber and a soft zone (low dislocation density) away from the fiber. The enhanced dislocation density in the copper matrix near the fiber arises because of the plastic deformation in response to the thermal stresses generated by the thermal mismatch between the fiber and the matrix. The intensity of the gradient in dislocation density will depend on the interfiber spacing. The dislocation density gradient will decrease with a decrease in the interfiber spacing. The existence of a plastically deformed zone containing high dislocation density in the metallic matrix near the reinforcement has also been confirmed by transmission electron microscopy by a number of researchers, both in fibrous and particulate metal matrix composites.

Thermal mismatch is indeed something that is difficult to avoid in any composite. By the same token, however, one can control the overall thermal expansion characteristics of a composite by controlling the proportion of reinforcement and matrix and the distribution of the reinforcement in the matrix. Many researchers have proposed models to predict the coefficients of thermal expansion of composites, determined experimentally these coefficients, and analyzed the general thermal expansion characteristics of metal matrix composites; we describe some of these in Chap. 10. It would be appropriate to point out here some special aspects of thermal characteristics of MMCs, especially particulate MMCs. This is because of their applications in electronic packaging, where their superior thermal characteristics play an important role; this makes it very important to understand the effects of thermal stresses and thermal cycling in MMCs. Prediction of CTE is complicated because of the structure of the composite (particles, whiskers, or fibers), interface, and the matrix plastic deformation due to internal thermal stresses. Expansion characteristics of isotropic composites are a function of V_{p} or V_{f}, size, and morphology of the reinforcement. Phenomena such as hysteretic deformation during thermal cycling, microcracking, and fiber intrusion on the surface lead to surface roughness. Rezai-Aria et al. (1993) observed surface roughness when they subjected Saffill fiber reinforced aluminum to thermal cycling. It is important to realize that the CTE of a material is not an absolute physical constant, but that it varies with temperature. This is especially so with MMCs, where the matrix can undergo plastic deformation as a result of thermal stresses (Vaidya and Chawla 1994). In addition, there are many microstructural factors that come into play. For example, a micromechanical analysis of the thermal expansion of two-dimensional $\mathrm{SiC}_p/\mathrm{Al}$ composites showed the importance of reinforcement continuity (Shen et al. 1994). Balch et al. (1996) investigated the role of reinforcement continuity on the thermal expansion of SiC/Al and the effect of the presence of voids on CTE. Their analysis showed that a high matrix yield strength, a high interfacial strength, and a convex reinforcement shape would minimize variations in CTE of a $\mathrm{SiC}_p/\mathrm{Al}$ type composite during any thermal excursion. In foam-reinforced composites, a weak interface could be exploited to produce void and thus minimize the average CTE of the composite, but hysteretic thermal expansion would be observed.

6.5.4 High Temperature Properties, Creep, and Fatigue

Superior high-temperature properties of MMCs have been demonstrated in a number of systems. For example, silicon carbide whiskers (SiC_w) improve the high-temperature properties of aluminum considerably. Figure 6.22 compares the elastic modulus, yield stress, and ultimate tensile strength of SiC$_w$ (21% V_f)/2024 Al composites to those of the unreinforced aluminum alloy (Phillips 1978). Figure 6.25 shows the fracture surface after tensile testing of a Nicalon fiber/aluminum composite at two temperatures. Note the more or less planar fracture with no fiber pullout at room temperature (Fig. 6.25a). At 500°C, a loss of adhesion between the fiber and the matrix occurs with the accompanying fiber/matrix separation and fiber pullout. The fiber pullout has left a hole in the center; see Fig. 6.25b.

High-modulus carbon fiber/aluminum composites combine a very high stiffness with a very low thermal expansion due mainly to the almost zero longitudinal

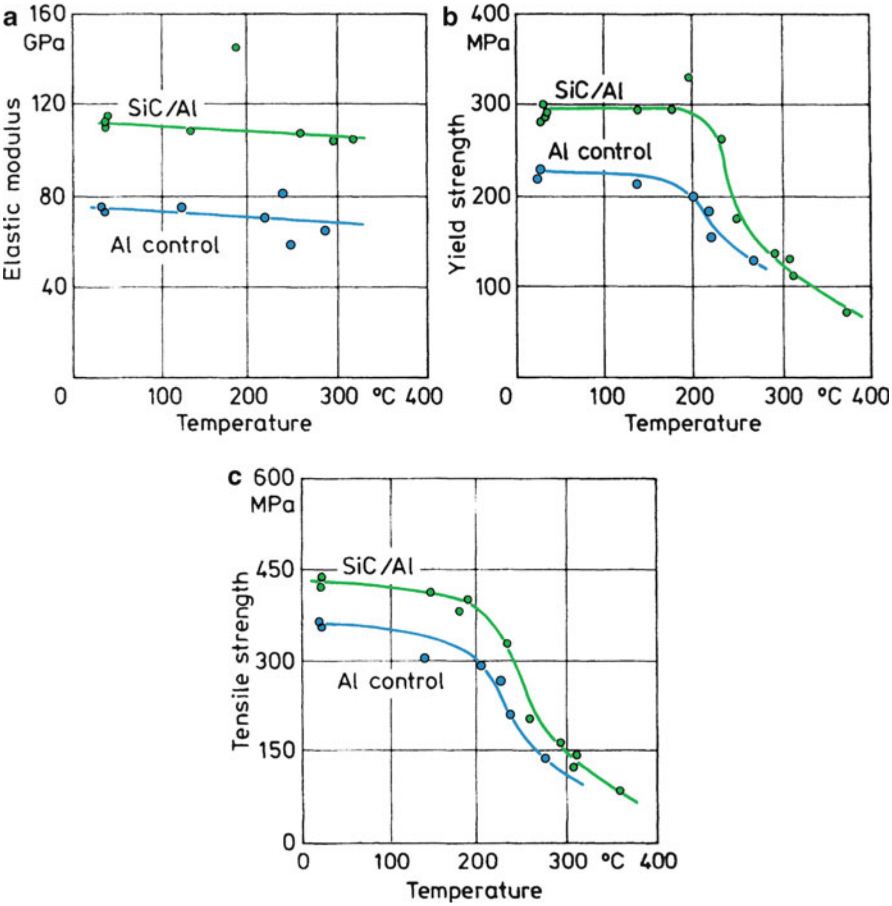

Fig. 6.24 Comparison of high-temperature properties of SiC$_w$/Al composites and aluminum: (**a**) elastic modulus, (**b**) yield stress, (**c**) ultimate tensile strength. [From Phillips (1978), used with permission]

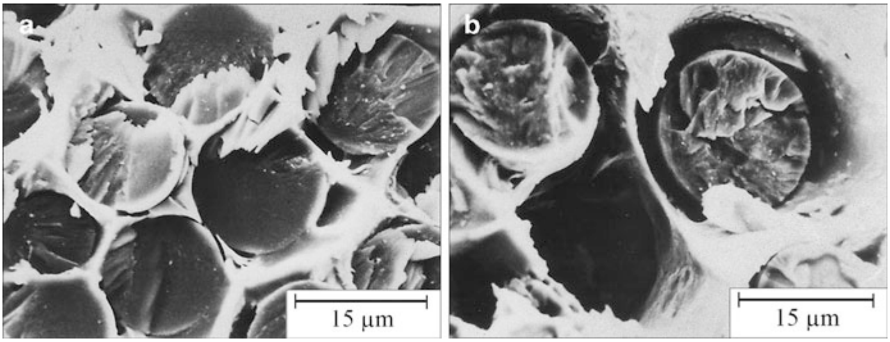

Fig. 6.25 Tensile fracture in Nicalon fiber/aluminum: (**a**) at room temperature showing a planar fracture, (**b**) at 500 °C showing fiber/matrix separation and fiber pullout leaving a hole. [Courtesy of K. Okamura]

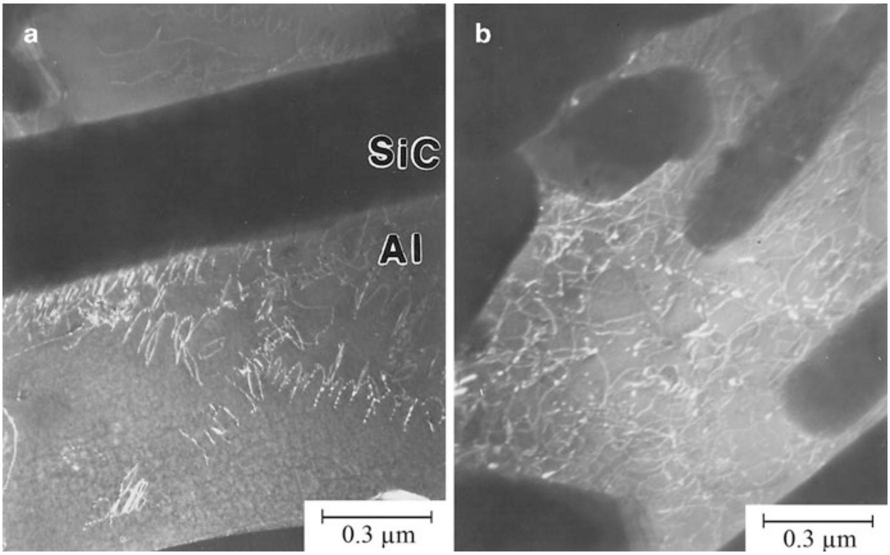

Fig. 6.26 Dislocation distribution in the aluminum matrix of a SiC_w/Al composite: (**a**) inhomogeneous dislocation distribution before testing, (**b**) uniform dislocation distribution after fatigue testing. [From Williams and Fine (1985a), used with permission]

expansion coefficient of carbon fibers. Carbon/aluminum composites, however, are susceptible to galvanic corrosion between carbon and aluminum. Carbon is cathodic in nature, while aluminum is anodic. Thus, galvanic corrosion can be a serious problem in joining aluminum to a carbon fiber composite. A common solution is to have an insulating layer of glass between the aluminum and the carbon composite. Any welding or joining involving localized heating could also be a potential source of problems because aluminum carbide may form as a result of overheating, which will be detrimental to the mechanical and corrosion properties.

The phenomenon of creep refers to time-dependent deformation. In practice, at least for most metals and ceramics, the creep behavior becomes important at high temperatures and, thus, sets a limit on the maximum application temperature. In general, this limit increases with the melting point of a material. We describe the creep behavior of MMCs along with that of other composites in Chap. 12.

Fatigue is the phenomenon of mechanical property degradation leading to failure of a material or a component under cyclic loading. Many high-volume applications of composite materials involve cyclic loading situations, e.g., automobile components. For a general discussion of fatigue behavior of composites, see Chap. 12. We mention here but one example of the importance of matrix microstructure on the fatigue behavior of MMCs. Williams and Fine (1985a) investigated the fatigue behavior of SiC whisker-reinforced 2124 Al alloy composites. Cyclic loading results in a uniform distribution of dislocations in the metal matrix. Figure 6.26 shows the dislocation distribution in an aluminum matrix before and after fatigue testing of a SiC_w/Al composite (Williams and Fine 1985a). Note the uniform dislocation distribution after fatigue testing. They found that unbonded SiC_p and non-SiC intermetallics were the fatigue crack-initiation sites. The unbonded SiC particles occur when clusters of SiC are present. Thus, not unexpectedly, reducing the clustering of SiC and the number and size of the intermetallics resulted in increased fatigue life.

6.6 Applications

It is convenient to divide the applications of metal matrix composites into aerospace and nonaerospace categories. In the category of aerospace applications, low density and other desirable features such as a tailored thermal expansion and conductivity and high stiffness and strength are the main drivers. Performance rather than cost is the important item. Inasmuch as continuous fiber reinforced MMCs deliver superior performance than particle reinforced composites, the former are frequently used in aerospace applications. In the nonaerospace applications, cost and performance are important, i.e., an optimum combination of these items is required. It is thus understandable that particle reinforced MMCs find more structural and nonstructural applications in nonaerospace fields. By far, the largest commercial application of MMCs is in the form of filamentary superconducting composites. We devote a whole chapter to such composites (Chap. 9) because of their commercial importance. Here, we provide a brief description of various other applications of MMCs.

Reduction in the weight of a component is a major driving force for any application in the aerospace field. For example, in the Hubble telescope, pitch-based continuous carbon fiber reinforced aluminum was used for waveguide booms because this composite is very light, has a high elastic modulus, E, and has a low coefficient of thermal expansion, α. Other aerospace applications of MMCs involve replacement of light but toxic beryllium. For example, in the US Trident missile, beryllium has been replaced by SiC_p/Al composite.

One of the important applications of MMCs in the automotive area is in diesel piston crowns (Donomoto et al. 1983). This application involves incorporation of short fibers of alumina or alumina + silica in the crown of the piston. The conventional diesel engine piston has an Al–Si casting alloy with crown made of a nickel cast iron. The replacement of the nickel cast iron by aluminum matrix composite resulted in a lighter, more abrasion-resistant, and cheaper product. Figure 6.27 shows a picture of such a piston; the arrow indicates the piston crown that is made of short fiber reinforced aluminum composite. Another application in the automotive sector involves the use of carbon fiber and alumina fibers in an aluminum alloy matrix for use as cylinder liners in the Prelude model of Honda Motor Co. Figure 6.28 shows the microstructure of the cylinder liner showing the unreinforced and fiber reinforced portions.

Continuous alumina fiber (Nextel 610)-reinforced Al composites are used to make power transmission cables. The cable consists of a composite core, consisting of Al_2O_3/Al composite wrapped with Al–Zr wires. The composite core bears most of the load as it has much higher stiffness and strength. Several tests were conducted on the actual conductor, including sag–tension behavior, vibration fatigue, thermal expansion, lightning resistance, and electrical resistance. Figure 6.29a shows these cables, while Fig. 6.29b shows the advantage in reducing the sag by using the 3M's Aluminum Conductor Composite Reinforced (ACCR) instead of the conventional aluminum-steel reinforced conductor (ACSR).

An important potential commercial application of particle reinforced aluminum composite is to make automotive driveshafts. In the design of a driveshaft, one needs to consider the speed at which it becomes dynamically unstable. It turns out that in terms of geometric parameters, a shorter shaft length and larger diameter will give a higher critical speed, N_c, while in terms of material parameters, the higher

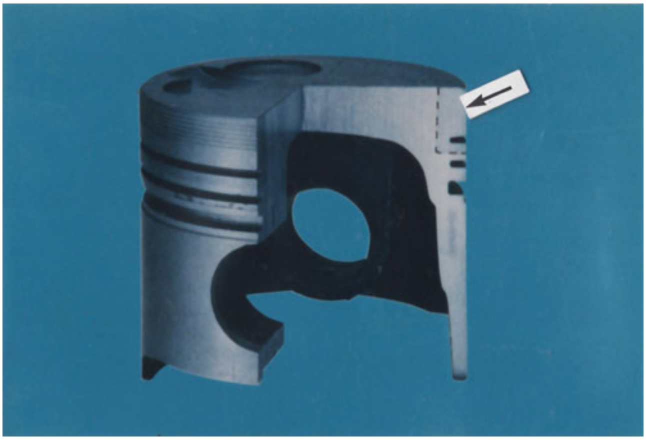

Fig. 6.27 A cutout of a squeeze cast piston with MMC inserts indicated by *dotted lines*. [Courtesy of Toyota Motor Co.]

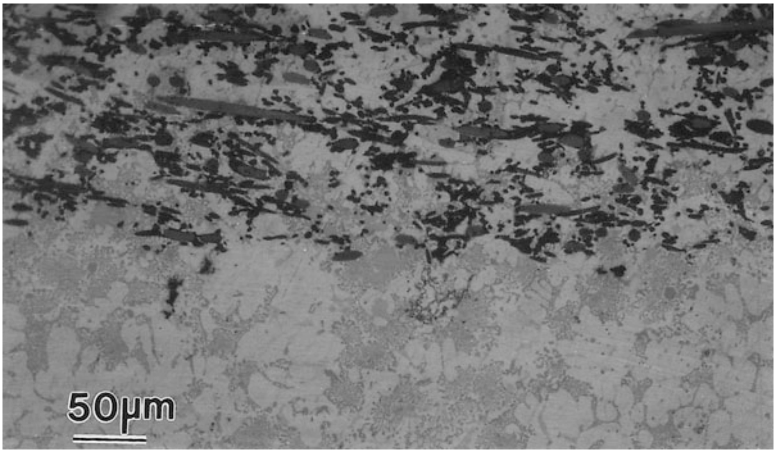

Fig. 6.28 Microstructure of the cylinder liner showing the unreinforced Al alloy (*bottom*) and fiber (alumina + carbon)-reinforced (*top*) portions

the specific stiffness (E/ρ), the higher N_c will be. One can make changes in the driveshaft geometry (increase the length or reduce the diameter) while maintaining a constant critical speed. A decrease in the driveshaft diameter can be important because of under-chassis space limitations.

Particulate metal matrix composites, especially with light metal matrix composites such as aluminum and magnesium, also find applications in automotive and sporting goods. In this regard, the price per kilogram becomes the driving force for application. An excellent example involves the use of Duralcan particulate MMCs to make mountain bicycles. A company, Specialized Bicycle in the United States, sells these bicycles with frames made from extruded tubes of 6061 aluminum containing about 10% alumina particles. The major advantage is the gain in stiffness.

An interesting example of a sheet laminate composite is a nonvibration sheet steel, made by Kawasaki Steel under the trade name Nonvibra™. A thin film of resin is sandwiched between two metal sheets. A chromate coating is applied on the inner surface of the skin metal. The chromate coating is conducive to cementing the bond between the resin and the outer skin metal. Such a laminated composite muffles noise over a broad range of frequencies, and it can be used in the temperature range of 0–100°C. Examples of applications include oil pans, locker covers, dashboard panels, floor panels, electrical machinery and appliances, and office equipment.

6.6.1 Electronic-Grade MMCs

Metal matrix composites can be tailored to have optimal thermal and physical properties to meet the requirements of electronic packaging systems (e.g., cores, substrates, carriers, and housings). Continuous boron fiber reinforced aluminum composites made by diffusion bonding have been used as heat sinks in chip carrier multilayer boards.

Fig. 6.29 (**a**) 3M's power transmission cables with composite core. (**b**) Reduction in sag by using the 3M's Aluminum Conductor Composite Reinforced (ACCR) instead of the conventional aluminum-steel reinforced conductor (ACSR). [Courtesy of 3M Corp.]

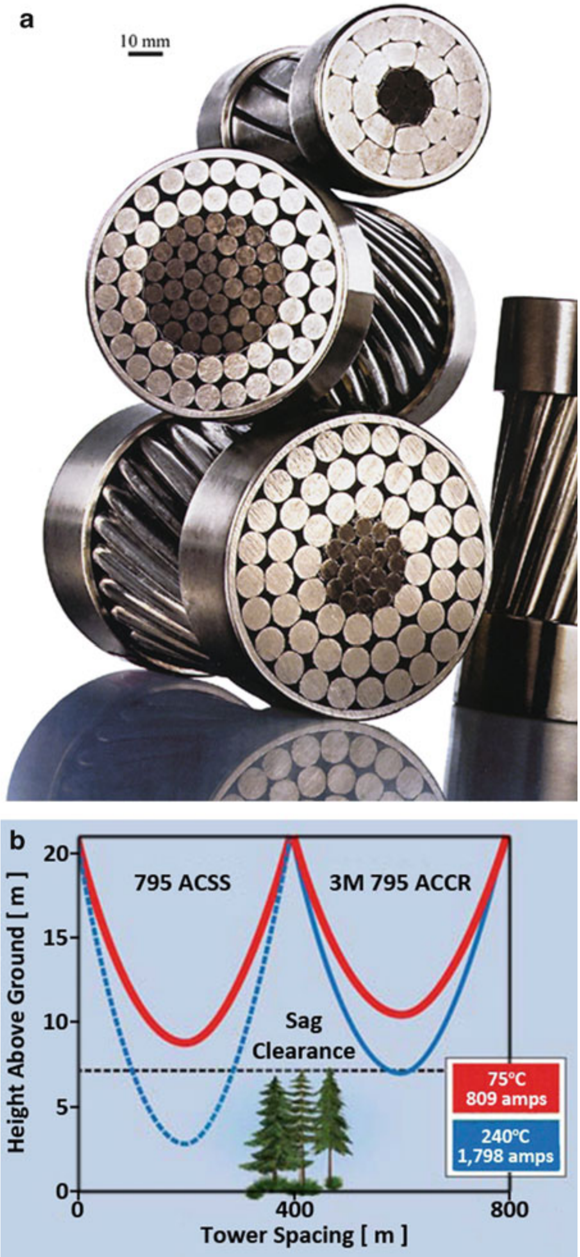

Unidirectionally aligned, pitch-based carbon fibers in an aluminum matrix can have very high thermal conductivity along the fiber direction. The conductivity transverse to the fibers is about two-thirds that of aluminum. Such a C/Al composite can find applications in heat transfer applications where weight reduction is an important consideration, for example, in high-density, high-speed integrated-circuit packages for computers and in base plates for electronic equipment. Can the reader think of a potential application in the disk drive of a computer?

Example Discuss the use of carbon fiber/copper matrix as a high-thermal-conductivity metal matrix composite for applications that require high thermal conductivity and high strength.

Answer Pitch-based carbon fibers can have very high thermal conductivity along the fiber axis, higher than even copper. Putting such fibers in a copper matrix will result in a high-strength, high-thermal-conductivity metal matrix composite. The problem with carbon fibers and metallic matrixes is that the surface energy considerations preclude wetting of the carbon fibers by the molten metals. The surface energy of carbon fiber is about 100 mJ/m^2, while most molten metals have surface energy of about 1,000 mJ/m^2. Recall from Chap. 2 that wetting occurs when the surface energy of the substrate (fiber) is higher than that of the molten metal. Thus, one does not expect the wetting of carbon fibers by molten copper. Two possible routes around this difficulty are as follows:

- Fiber surface modification
- Matrix modification

It would appear that modification of carbon fiber surface by making it rough could result in a reasonable mechanical bond between carbon fiber and copper matrix.

6.6.2 Recycling of Metal Matrix Composites

Particle reinforced metal matrix composites such as SiC_p/Al or Al_2O_3/Al are more cost-effective than continuous fiber reinforced MMCs such the ones reinforced with C, SiC, or Al_2O_3 fibers. There are two main reasons for this: the cost of continuous fiber and the cost of processing the composite. Also, secondary fabrication (extrusion, forging, rolling, etc.) is very difficult with continuous fiber reinforced composites MMCs. One of the problems of recycling of composites made of alumina or silicon carbide particles in an aluminum matrix is that a mass of unreinforced aluminum is indistinguishable from a mass of reinforced aluminum. The ultimate objective is always to obtain a part or component that performs a function in a cost-effective manner.

There are two aspects of recycling MMCs (Schuster et al. 1993; Lloyd 1994; Nishida 2001):

- Recycling of MMCs as MMCs, i.e., without separating the reinforcement from the matrix. This can be quite economical where it is possible to use. One should

Fig. 6.30 Chemical action of fluxing materials to separate the metal matrix from fiber or particle [after Nishida 2001]

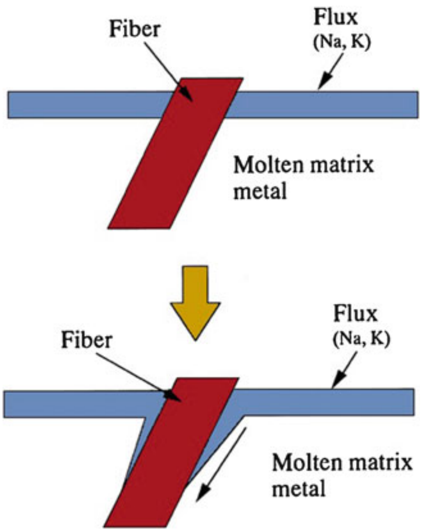

be mindful of certain steps in such a reuse of MMCs. One should avoid excessive use of treatments involving thermal excursions or lengthy thermal exposures, because they can cause adverse chemical interactions at the interface. Some aluminum metal matrix composites can be recycled and reused, especially if the Si content is sufficient to retard formation of aluminum carbide, which is highly deleterious to mechanical properties. Addition of virgin metal to the reinforced material to obtain a composite with a desired particle volume fraction may be required.

- Recovery or reclamation of the original components by separating them via the use of fluxing materials that have lower surface energies with the ceramic reinforcement than with the metal matrix is a viable option. This is similar to tertiary recycling of PMCs (see Chap. 5), i.e., one attempts to recover the original components. There are two ways to do this: mechanical or chemical. Various mechanical methods of separating the metal and ceramic particles, such as crushing, shredding, and gravity separation, can be used. Chemical techniques involve the use of fluxing materials. These fluxing materials should have lower surface energies with the ceramic reinforcement than with the metal matrix. Al can be reclaimed from scrap by melting at 700°C, and by adding salt and bubbling argon through the melt to form froth that concentrates alumina and SiC particles dewetted by the salt. Figure 6.30 show this process of chemical separation via fluxing. Using combined argon and salt fluxes, silicon carbide particles can be removed from the melt and 85–90% of the aluminum can be reclaimed (Lloyd 1994).

References

Aghajanian MK, Burke JT, White DR, Nagelberg AS (1989) SAMPE Quart 34:817–823

Arsenault RJ, Fisher RM (1983) Scr Mater 17:67

Arsenault RJ, Shi N (1986) Mater Sci Eng 81:175

Baker AA, Shipman C (1972) Fibre Sci Technol 5:282

Balch DK, Fitzgerald TJ, Michaud VJ, Mortensen A, Shen Y-L, Suresh S (1996) Metall Mater Trans A 27A:3700

Barrera EV, Sims J, Callahan DL, Provenzano VJ, Milliken J, Holtz RL (1994) J Mater Res 9:2662

Beck Tan NC, Aikiri, Jr. RM, Briber RM (1994) Met Mater Trans 25A:2461

Champion AR, Krueger WH, Hartman HS, Dhingra AK (1978). In: Proceedings of International Conference on Composite Materials (ICCM/2). TMS-AIME, New York, p 883

Chawla KK (1973a) Metallography 6:155

Chawla KK (1973b) Philos Mag 28:401

Chawla KK (1974) In: Grain boundaries in engineering materials. Claitor's, Baton Rouge, p 435

Chawla KK (1975) Fibre Sci Technol 8:49

Chawla KK (Dec., 1985) J Metals 37:25

Chawla KK (1989) In: Precious and rare metal technologies. Elsevier, Amsterdam, p 639

Chawla KK, Collares CE (1978). In: Proceedings of the 1978 International Conference on Composite Materials (ICCM/2), TMS-AIME, New York, p 1237

Chawla KK, Metzger M (1972) J Mater Sci 7:34

Chawla KK, Metzger M (1978) In: Fracture 1977. In: Proceedings of the 4th international conference on fracture, vol 3, Pergamon Press, p 1039

Chawla KK, Esmaeili AH, Datye AK, Vasudevan AK (1991) Scr Mater et Mater 25:1315

Chawla N, Andres C, Jones JW, Allison JE (1998) Metall Mater Trans 29A:2843

Christman T, Suresh S (1988) Mater Sci Eng A102:211

Christodolou L, Parrish PA, Crowe CR (1988) In: Mater Res Soc Symp Proc 120:29–34

Cline HE, Walter JL, Koch EF, Osika LM (1971) Acta Mater 19:405

Cook AJ, Warner PS (1991) Mater Sci Eng A144:189

Cornie JA, Chiang Y-M, Uhlmann DR, Mortensen AS, Collins JM (1986) Ceram Bull 65:293

Divecha AP, Fishman SG, Karmarkar SD (Sept., 1981) J Metals 9:12

Donomoto T, Miura N, Funatani K, and Miyake N (1983). SAE Techical Paper No. 83052, Detroit, MI

Dunand DC, Mortensen A (1991a) Acta Metall Mater 39:127

Dunand DC, Mortensen A (1991b) Acta Metall Mater 39:1405

Dutta I, Bourell DL (1988) Mater Sci Eng A112:67

Dutta I, Bourell DL (1990) Acta Metall 38:2041

Dutta I, Bourell DL, Latimer D (1988) J Compos Mater 22:829

Fu L-J, Schmerling M, Marcus HL (1986) In: Composite materials: fatigue and fracture, ASTM STP 907. ASTM, Philadelphia, 51

Fujiwara C, Yoshida M, Matsuhama M, Ohama S (1995). In: Proceedings of International Conference on Composite Materials (ICCM-10), p II–687.

Gabryel CM, McLeod AD (1991) Metall Trans 23A:1279

Ghosh AK (1993) In: Metal matrix composites. Butterworth-Heinemann, Boston, p 119

Hill RG, Nelson RP, Hellerich CL (1969). In: Proceedings of the 16th refractory working group meeting, Seattle, WA

Hunt WH, Osman TM, Lewandowski JJ (1993) JOM 45:30

Isaacs JA, Taricco F, Michaud VJ, Mortensen A (1991) Metall Trans 22A:2855

Jones C, Kiely CJ, Wang SS (1993) J Mater Res 4:327

Katzman HA (1987) J Mater Sci 22:144

Kerans RJ, Parthasarathy TA (1991) J Am Ceram Soc 74:1585

Kohyama A, Igata N, Imai Y, Teranishi H, Ishikawa T (1985). In: Proceedings of the fifth International Conference on Composite Materials (ICCM/V), TMS-AIME, Warrendale, PA, p 609

Lloyd DJ (1994) Int Mater Rev 39:1

Majidi AP, Chou TW (1987) Proc Int Conf Compos Mater VI 2:422

Manning C, Gurganus T (1969) J Am Ceram Soc 52:115

Manoharan M, Lewandowski JJ, Hunt WH (1993) Mater Sci Eng A17:63

McDanels DL (1985) Metall Trans 16A:1105

McLean M (1983) Directionally solidified materials for high temperature service. The Metals Soc, London

Mehrabian R, Riek RG, Flemings MC (1974) Metall Trans 5:1899

Meyerer W, Kizer D, Paprocki S, Paul H (1978). In: Proceedings of the 1978 International Conference on Composite Materials (ICCM/2), TMS-AIME, New York, p 141

Meyers MA, Chawla KK (1984) Mechanical metallurgy. Prentice-Hall, Englewood Cliffs, 494

Michaud VJ (1993) Metal matrix composites. Butterworth-Heinemann, Boston, p 3

Mitra R, Chiou WA, Fine ME, Weertman JR (1993) J Mater Res 8:2300

Mortensen A, Gungor MN, Cornie JA, Flemings MC (1986) J Metals 38:30

Mortensen A, Cornie JA, Flemings MC (1988) J Metals 40:12

Nardone VC, Prewo KM (1986) Scr Mater 20:43

Naslain R, Thebault J, Pailler R (1976). In: Proceedings of the 1975 International Conference on Composite Materials, vol 1, TMS-AIME, New York, p 116

Nieh TG, Karlak RF (1984) Scr Mater 17:67

Nishida Y (2001) Adv Eng Mater 3:315

Nourbakhsh S, Liang FL, Margolin H (1990) Metall Trans A 21A:213

Parrini L, Schaler R (1994) J Alloy Comp 211:402

Partridge PG, Ward-Close CM (1993) Int Mater Rev 38:1

Pennander L, Anderson C-H (1991) In: Hansen N et al. (eds) Metal matrix composites – Processing, microstructure and properties. 12th Risø international symposium on materials science, p 575

Pfeifer M, Rigsbee JM, Chawla KK (1990) J Mater Sci 25:1563

Phillips WL (1978). In: Proceedings of the 1978 International Conference on Composite Materials (ICCM/2), TMS-AIME, New York, p 567

Rack HJ (1987). In: Sixth International Conference on Composite Materials, Elsevier Applied Science, New York, p 382

Rezai-Aria F, Liechti T, Gagnon G (1993) Scr Metall Mater 28:587

Rhee S (1970) J Am Ceram Soc 53:386

Rohatgi PK, Asthana R, Das S (1986) Int Met Rev 31:115

Schuster DM, Skibo MD, Bruski RS (1993) J Miner Met Mater Soc 45(5):26

Shen Y-L, Needleman A, Suresh S (1994) Metall Mater Trans A 25A:839

Sherby O, Lee S, Koch R, Sumi T, Wolfenstine J (1985) Mater Manuf Process 5:363

Shi N, Arsenault RJ (1991) J Compos Technol Res 13:211

Shi N, Arsenault RJ (1993) Metall Trans 24A:1879

Srivatsan TS, Lavernia EJ (1992) J Mater Sci 27:5965

Suresh S, Chawla KK (1993) In: Metal matrix composites. Butterworth-Heinemann, Boston, p 119

Thomas DG (1965) J Colloid Sci 20:267

Vaidya RU, Chawla KK (1994) Compos Sci Technol 50:13

van Suchtelan J (1972) Philips Res Rep 27:28

van Suchtelen J (1972) Philips Res Rep 27:28

Vasudevan AK, Doherty RD (eds) (1989) Aluminum alloys – Contemporary research and applications. Academic, Boston

Vasudevan AK, Petrovic JJ (eds) (1992) High temperature structural silicides, Elsevier, Amsterdam

Walter JL (1982) In situ composites IV. Elsevier, New York, p 85

Warren R, Andersson C-H (1984) Composites 15:101
Williams DR, Fine ME (1985a). In: Proceedings of the 5th International Conference on Composite Materials (ICCM/V), TMS, Warrendale, PA, p 275
Williams DR, Fine ME (1985b). In: Proceedings of the Fifth International Conference on Composite Materials (ICCM/V), TMS-AIME, Warrendale, PA, p 369

Further Reading

Chawla N, Chawla KK (2006) Metal matrix composites. Springer, New York
Clyne TW, Withers PJ (1993) An introduction to metal matrix composites. Cambridge University Press, Cambridge
Mortensen A, Llorca J (2010) Annu Rev Mater Res 40:243
Suresh S, Needleman A, Mortensen A (eds) (1993) Metal matrix composites. Butterworth-Heinemann, Boston
Taya M, Arsenault RJ (1990) Metal matrix composites. Pergamon, Oxford

Problems

6.1. Pressure casting is frequently used to prepare metal matrix composite. Explain why.
6.2. Describe some of the advantages of metal matrix composites over monolithic metals.
6.3. Discuss the advantages of metal matrix composites vis à vis polymer matrix composite.
6.4. Discuss the advantages and disadvantages of liquid metal processing vis à vis other methods of fabricating metal matrix composites.
6.5. Silicon carbide (0.1 μm thick) coated boron fiber was used to reinforce a metallic matrix. The SiC coating serves as a diffusion barrier coating. Estimate the time for dissolution of this coating at 700 K if the diffusion coefficient at 700 K is 10^{-16} m^2/s.
6.6. The metallic matrix will generally undergo constrained plastic flow in the presence of a moderately high volume fraction of high modulus fibers. Draw schematically the stress–strain curves of a constrained metal matrix (i.e., in situ behavior) and an unconstrained metal (i.e., 100% matrix metal). Explain the difference.
6.7. Aluminum and magnesium are two common metal matrix materials. What is the viscosity of molten aluminum and magnesium?

6.8. What is the effect on viscosity of adding ceramic particles to a molten metal such as aluminum or magnesium? Discuss its implications in the processing of MMCs with respect to features such as particle size, volume fraction, etc.

6.9. Discuss the problem of thermal stability of unidirectionally solidified eutectic (in situ) metallic composites.

6.10. Discuss the use of silicon carbide particle reinforced aluminum composites in braking applications.